

Thesis

**Association of PKC Gamma Missense SNP with HCV Induced
Hepatocellular Carcinoma**



By

TALHA IQBAL

Reg NO. 00000317897

MS Healthcare Biotechnology 2019-2021

Supervisor

Dr. MARIA SHABBIR

**Attar-UR-Rahman School of Applied Biosciences, National University of
Sciences & Technology, Islamabad, Pakistan**

2021

Declaration

I hereby declared that except where Specific reference is made to the work of others, the content of this dissertation is original and have not been submitted in whole or in part for consideration for any other degree or qualification in this or any other University. This dissertation is the result of my own work and includes the outcome of the work done.

Talha Iqbal

Table of Contents	v
List of tables	vi
List of figures	vii
List of abbreviations	viii

Table of contents

Abstract	1
1 INTRODUCTION	2
1.1 Single Nucleotide Polymorphism (SNP).....	2
1.2 Liver Cancer	3
1.3 Maytansine	4
2 Literature Review	6
2.1 Cancer.....	6
2.2 Protein Kinase C.....	8
2.3 Maturation	9
2.4 Activation	9
2.5 Role of Calcium Ions Fatty Acids	10
2.6 Protein Kinase C Gamma	10
2.7 Role of PKC Gamma in Cancer	12
2.8 PKC Gamma Signalling	16
2.9 PKC gamma and its interacting partners	16
2.10 PKC Gamma Inhibitors	18
2.10.1 Enzastaurin	18
2.10.2 Staurosporine.....	19

2.10.3 Bisindolylmaleimides	19
2.10.4 Midostaurin	19
3 Methodology	21
3.1 Structure Prediction of PKC gamma	22
3.2 Uniqueness and Localization	22
3.3 Retrieval & Identification of Pathogenic snps	22
3.4 Structural and Functional Analysis	23
3.5 Molecular Dynamic Simulations.....	24
3.6 Protein Docking.....	24
3.7 Primer Designing.....	25
3.8 Genomic DNA Extraction	25
3.9 Polymerase Chain Reaction	26
3.10 PCR Steps and Conditions	27
3.11 PCR Mixture Preparation	27
3.12 Gel Electrophoresis	27
3.13 Agarose gel preparation	28
3.14 ALT/SGPT Test	28
3.15 Viral RNA Extraction.....	29
3.16 qRT-PCR.....	29
4 Results	31
4.1 Structure of PKC Gamma	31
4.2 Phylogenetic Tree and Subcellular Localization.....	32
4.3 Damaging SNPs	33
4.4 Effect Of nsSNPs on PRKCG Structure and Function	35
4.5 MD Simulation Results	37
4.5.1 RMSD Analysis.....	37
4.5.2 RMSF Analysis	38

4.5.3 Radius of Gyration	39
4.5.4 Number of Hydrogen Bonds	40
4.6 AdmetSAR Analysis of a Drug	41
4.6.1 Lipinski's Rule of Five.....	41
4.6.2 Regression Analysis	41
4.6.3 ADMET Properties	42
4.7 Interpretation of Protein-ligand Interaction	43
4.8 Genotype Data of HCC And Control Samples.....	45
4.8.1 Data Based on Gender	46
4.8.2 Age Group Data	47
4.9 Analysis of ALT In Patient vs Control.....	48
4.10 Viral Load Analysis of Patients with Different Alleles	49
5. Discussion	50
5.1 Conclusion.....	53
References	55

List of Tables

1. Different PKC inhibitors, their structures, mechanism of action, half maximal inhibitory concentration (CI50) along with the references	20
2. List of different computational tools that were used to predict pathogenicity of nsSNPs, their scoring criteria and classification.	23
3. Pathogenic nsSNPs based on six different tools.	34
4. Filtered nssnps after applying filters.	35
5. I-Mutant Effect of nsSNPs on protein stability	36.
6. List of possible alteration in the protein when lysine is changed with arginine at 359 position and their P-values estimated by mutpred2.....	36
7. Physio-chemical properties of the drug and their values predicted by AdmetSAR.	41
8. Regression properties predicted by AdmetSAR.....	42
9. Pharmacokinetic properties of the drug.....	42
10. CB Dock table representing possible interaction score and cavity size.	43
11. Genotype Data of Patient and Control	45
12. Allelic Data Based on Gender	46
13. Allelic Data of Different Age Groups	47

List of Figures

1. Different steps in cancer metastasis three main process i.e., Intravasation (Released of tumor form its primary site and intravasate blood stream), Escape form immune surveillence and finally extravasation of tumor cells to other sites 7
2. Schematic diagram of PKC gamma representing different domains of the protein i.e., PE/DAG domain, C2 domain and kinase domain and their functions 9
3. Diagrammatic representation of cPKC maturation and Activation. (i) Shows newly synthesized protein with exposed Pseudosubstrate site at N-terminal, (ii) Hsp90 dependent phosphorylation of kinase domain via mtorc2/PDK-1 (iii) Ca²⁺ dependent translocation to plasma membrane (iv) binding of protein with DAG and downstream signaling (v) re-prephosphorylation of protein to sustain its singling lifetime..... 12
4. Schematic diagram of PKC signaling shows the role of cpkc and nPKC in different types of cell processes i.e., Cell proliferation, differentiation, apoptosis, and cell polarity, etc 15
5. Schematic representation of PKC signaling, its interaction partners i.e., proteins of MAPK pathway, NF-K β beta pathway, etc. And its role in gene regulation..... 18
6. Flow chart of different in-silico methods that were followed in this study....21
7. Workflow of In-vitro methodology..... 21
8. Model 3 of PKC gamma predicted via I-TASSER with C-score (-0.53). The protein structure is colored in green, and domains are highlighted in different colours. DAG domain (red color), C2 domain (blue), kinase domain (yellow) and AGC kinase (magenta) 30
9. Localization route of the PKC gamma protein along with the probability score. The red line shows the path of localization32
10. Represents the Phylogenetic Tree of the PKCs proteins. All the PKCs are originated from common root and then evolute into three different classes i.e., cPKCs, nPKCs and aPKCs.....33
11. Graphical representation of PRKCG SNPs..... 34

12. Lysine on the right side which in mutated to arginine located on the left side. The size of arginine is larger from lysine as two extra NH groups attachment....	37
13. 11 RMSD graph representing the significance difference in the deviation pattern between wild and mutated protein over the time	38
14. Amino acid residues of both wild and mutated protein was plot on x-axis against RMSF values on y-axis to analyse the difference in the fluctuation of both proteins from the reference point	39
15. Radius of gyration of both wild and mutated protein shows the compactness of protein in a dynamic setting as the simulation proceeds.....	40
16. Represents the difference in the number of hydrogen bonds between wild and mutated protein.....	40
17. Shows the drug binding pocket of the receptor in surface form and the attached ligand in sticks and balls format	44
18A. Protein-ligand bonding and molecular interaction. Amino acid with hydrophobic interaction, Hydrogen bonding, covalent bonding ligand and non-ligand, distance of hydrogen bonding are shown in semi-spiked circle, green dotted lines, orange, and purple lines, angstrom (3.13 & 2-91) and carbon, nitrogen and oxygen molecules are represented in black, blue, and red circles	44
18B. 3d representation of protein-ligand bonding via pymol	45
19. Comparison of ALT concentration in patients and control.....	48
20. Correlation of viral load and Genotype.....	49

List of Abbreviations

AD	Accessory Domain
ADMET	Absorption Distribution Metabolism Excretion and Toxicity
AFP	Alpha Fetoprotein
ALT	Alanine Transaminase
AMPK	AMP-activated Protein Kinase
aPKC	Atypical Protein Kinase C
ARMS	Amplification-refractory Mutation System
ATP	Adenosine Triphosphate
AXL	AXL Receptor Tyrosine Kinase
CADD	Combined Annotation Dependent Depletion
CASP	Critical Appraisal Skills Programme
CI	Confidence Interval
cPKC	Conventional Protein Kinase C
CT	Cycle Threshold
DAG	Diacylglycerol
DNA	Deoxyribonucleic Acid
EDTA	Ethylenediaminetetraacetic Acid
EGFR	Epidermal Growth Factor Receptor
EMT	Epithelial–Mesenchymal Transition

ERK	Extracellular signal-regulated Kinase
FASTA	FAST-All
FATHMM	Functional Analysis through Hidden Markov Models
GP73	Golgi Protein 73
GWAVA	Genome Wide Annotation of VARIants
HCC	Hepatocellular Carcinoma
HCV	Hepatitis C Virus
HOPE	Have Our Protein Explained
iCCA	Intrahepatic Cholangiocarcinoma
IL-28B	Interleukin 28B
I-TASSER	Iterative Threading ASSEmbly Refinement
KIF1B	Kinesin Family Member 1B
LEDGF	Lens Epithelium-derived Growth Factor
MAPK	Mitogen-activated protein kinase
MD	Molecular Dynamics
MDM2	Mouse double minute 2
MDR	Multi-Drug Resistance
MICA	MHC Class I Polypeptide-Related Sequence A
MM	Multiple Myeloma
mTORC2	Mammalian Target of Rapamycin Complex 2
NF- κ B	Nuclear Factor Kappa Light Chain Enhancer of Activated B cells

nPKC	Novel Protein Kinase C
NSCLC	Non-small Cell Lung Cancer
OR	Odd Ratio
P53	Protein 53
PCR	Polymerase Chain Reaction
PDB	Protein Data Bank
PDG	Phosphogluconate Dehydrogenase
PDGFR	Platelet-Derived Growth Factor
PK-1	Phosphoinositide-dependent Kinase-1
PE	Proboscis Ester
PKC	Protein Kinase C
PLC	Phospholipase C
PNPLA3	Patatin-like phospholipase domain-containing protein 3
PS	Phosphoserine
RACK	Receptor for activated C kinase
RI	Reliability Index
RMSD	Root Mean Square Deviation
RMSF	Root Mean Square Fluctuation
RNA	Ribonucleic Acid
RR	Relative Risk
RTK	Receptor Tyrosine Kinase

SDF	Standard Data Format
SDS	Sodium Dodecyl Sulphate
SFTP	Secure File Transfer Protocol
SGPT	Serum Glutamic Pyruvic Transaminase
SMILES	Simplified Molecular Input Line Entry System
SNP	Single Nucleotide Polymorphism
TAE	Tris-acetate-EDTA
TE	Tris-EDTA
TGF- β -1	Transforming growth factor beta 1
UBE4B	Ubiquitination Factor E4B
UV	Ultraviolet

Association of Missense SNP in PKC Gamma with HCV Induced Hepatocellular Carcinoma

Abstract

The primary liver cancer also referred as Hepatocellular carcinoma (HCC), is a lethal disease accounts for approximately 90% of liver cancer worldwide. The major problem with HCC is early diagnosis. PKC gamma a member of conventional PKC involved in many cancers type but in context of single nucleotide polymorphism the protein was not much explored. The in-silico investigation of PKC gamma SNPs via edictSNP, 2021, CADD, DANN identify missense pathogenic mutation (K359R) rs1331234028. The AA variant of this genotype shows strong association with HCC. The odd ratio (OR) and relative risk (RR) for this variant was 5.194 and 2.287 respectively, having 0.0001 P-value. In-silico structural and functional analysis predict that upon this mutation the protein stability may decrease. For therapeutic purpose Maytansine was docked with PKC gamma which shows promising results and can be used as inhibitor of PKC gamma. The genetic variation in PKC gamma can be helpful in the early diagnosis of the hepatocellular carcinoma.

Chapter 1 Introduction

1.1 Single Nucleotide Polymorphism (SNP)

Human genome possesses various types of variation, but the amplest among these variations are single nucleotide polymorphisms (SNPs). There are roughly about 3-10 million SNPs which comprises almost 1% of the whole genome (Wright, 2001). Non-synonymous SNP (nsSNPs) /missense SNPs residing in the coding region are very crucial and accounts for residual change which may have neutral or deleterious effect on protein (Capriotti & Altman, 2011) (F. S. Collins, Guyer, & Chakravarti, 1997). These variations may account for some damaging effects i.e. protein structure destabilization, aberrant gene regulation (Barroso et al., 1999), alteration in protein hydrophobicity, proteins charge disturbance, change in protein geometry (Petukh, Kucukkal, & Alexov, 2015), altered stability, dynamics, translation, protein-protein interactions (Chasman & Adams, 2001) (Kucukkal, Petukh, Li, & Alexov, 2015) and loss of protein integrity (Thomas et al., 1999). SNPs are present in almost every region of the gene and can act as susceptibility or causative factor in cancer. Polymorphism in the genes of cell cycle regulation, DNA repair system, genes involve in immune regulation and metabolic associated genes can lead to cancer development (Devilee & Rookus, 2010) (He et al., 2015; Jing, Li, & Yuan, 2012). Genetic analysis determined the association of SNPs with HCC development. Genome wide association study (GWAS) identified thousands of SNPs in different genes i.e., IL-28B, PNPLA3, KIF1B, PGD, UBE4B, MICA, MDM2, P53 and several other genes that were found to be associated with hepatocellular carcinoma (HCC) (Yoon et al., 2008) (Balagopal, Thomas, & Thio, 2010) (Kumar et al., 2011) (Nahon & Zucman-Rossi, 2012).

1.2 Liver cancer

The primary liver cancer also referred as Hepatocellular carcinoma (HCC), is a lethal disease accounts for approximately 80% of liver cancer worldwide with high prevalence in Asia and Africa (Jemal et al., 2011) (S Darvesh, B Aggarwal, & Bishayee, 2012). Life expectancy of HCC is stage dependent ranges from few months to almost five years as at which stage the cancer is diagnosed. Poor prognosis in HCC just like any other cancer is largely because of the late diagnosis at advanced stages when traditional chemotherapy become no more effective (Forner, Llovet, & Bruix, 2012) (Y. R. Liu et al., 2015). Intrahepatic Cholangiocarcinoma (iCCA) another types of primary liver cancer accounts for approximately 10% of all the Cholangiocarcinoma and arise in every 2-3 individuals per 100,000 in west and occurs a bit more in men than women. In Asia it is more common in People's Republic of China and Thailand with 10 and 71 cases per 100,000, respectively (Shin et al., 2010) (Tyson & El-Serag, 2011) (Khan, Toledano, & Taylor-Robinson, 2008). The aberrated cascade of complex signaling is involved in progression of hepatocarcinogenesis. The genetic standpoint of the disease will be heterogenous if it occurs because of incrimination of several signaling pathways.

Other major types of liver cancer are bile duct cystadenocarcinoma, combined hepatocellular and cholangiocarcinoma, hepatoblastoma and undifferentiated carcinoma. All these types of cancer are categories based on the tissue they originate. The major problem with Liver cancer especially hepatocellular carcinoma is the diagnosis of the disease in early stage. In majority cases of hepatocellular carcinoma diagnosed patients it was found that the cancer has already

been metastasized and resistant to therapy (Chedid et al., 2017). Several diagnostic biomarkers i.e., Alpha fetoprotein (AFP), AXL Receptor Tyrosine Kinase (AXL), Thioredoxin, Golgi protein 73 (GP73) and Annexin A2 has been used for the diagnosis of hepatocellular carcinoma but the is unable to solve the problem of early cancer detection (Chia, Wong, & Luk, 2019).

The genetic polymorphism involved in PKC gamma affect its protein structure and hence its function. Missense SNPs in the PKC gamma may increase the likelihood or susceptibility of hepatocellular carcinoma progression or development. The main aim of this study is to identify and analysis the most pathogenic non-synonymous SNPs in PKC gamma which has direct impact on protein 3D structure. The SNPs identified were further analyzed to establish the association of those damaging SNPs with the liver cancer. The role of PKC gamma in the development and progression is well establish. Several studies determined that the PKC gamma is associated with cancer at different stages i.e., glioma, kidney cancer, colon cancer and liver cancer etc. However, all those studies established the role of PKC gamma progression, development, its differential expression in various cancers but these studies do not provide sufficient information about the role of genetic polymorphism and its association with carcinogenesis. PKC gamma a member of PKC family located on chromosome 19 at position 19q13.2-q13.4. The activation of PKC gamma depends on calcium and diacylglycerol (DAG) (Lisa Coussens et al., 1986). The information gathered in this study about the polymorphism in PKC gamma, structural and functional analysis of the missense SNP and In-vitro study can help us to determine new potential genetic marker and drug target site for therapeutic intervention.

1.3 Maytansine

Maytansine, an alcoholic plant extract isolated from *Maytenus ovatus*, has been found to have potential cytotoxic and anticancer activity. The discovery of Maytansine's anticancer activity grabbed the attention and seeking for its new sources was prompted. The initial results of Maytansine as anticancer drug were not promising, but later the conjugation of the drug with different antibodies i.e., C242, CD19 and He2 has shown high efficacy and improved safety in different cancers.

Chapter 2 Literature Review

2.1 Cancer

Cancer, a group of disease cause due to the mutation in DNA, RNA or protein which results in deregulated cell division and in turn tumor formation and escape from the primary site and invade other cells as well. Cell cycle in normal cells is tightly regulated at different checkpoints which ensure that cell is ready and there is no defect in it to move from one phase to another. The disruption of these regulators can leads to cancer development, uncontrolled proliferation and invasion (G. I. Evan & Vousden, 2001). The evolutionary analysis of the cancer provides a deep insight regarding tumor development and tumorigenesis. These studies show the rarity of cancer cells, approximately 1 in 2×10^7 mutation per gene cell division (Oller, Rastogi, Morgenthaler, & Thilly, 1989). The huge repertoire of genes that are involved in the regulation of cell division from their early development to maturation and then expansion and statistical analysis that revealed that cancer may occur 1 in 3 lifetimes shows the significant role of anti-tumor mechanism and also demonstrated that defect in these mechanism can leads to cancer (G. Evan & Littlewood, 1998). In the cancer development two categories of genes are very much important, one is oncogenes and second one is tumor suppressor genes. These Proteins of these two categories work in an antagonistic manner i.e., oncogenes' product is involved in the induction of cancer while the tumor suppressor proteins play role in tumor suppression. These proteins are of different nature as they maybe a growth factor or their receptor, second messenger proteins, DNA binding proteins or maybe some other proteins (Klein, 1988). As it is seen in many cancers that they do not remain benign rather invade other cells and tissue away from the primary tumor site and become malignant via metastasis. Metastasis is a multistep

process depends on the microenvironment of tumor, invasion, motility, angiogenesis and colonization etc. (Gupta & Massagué, 2006).

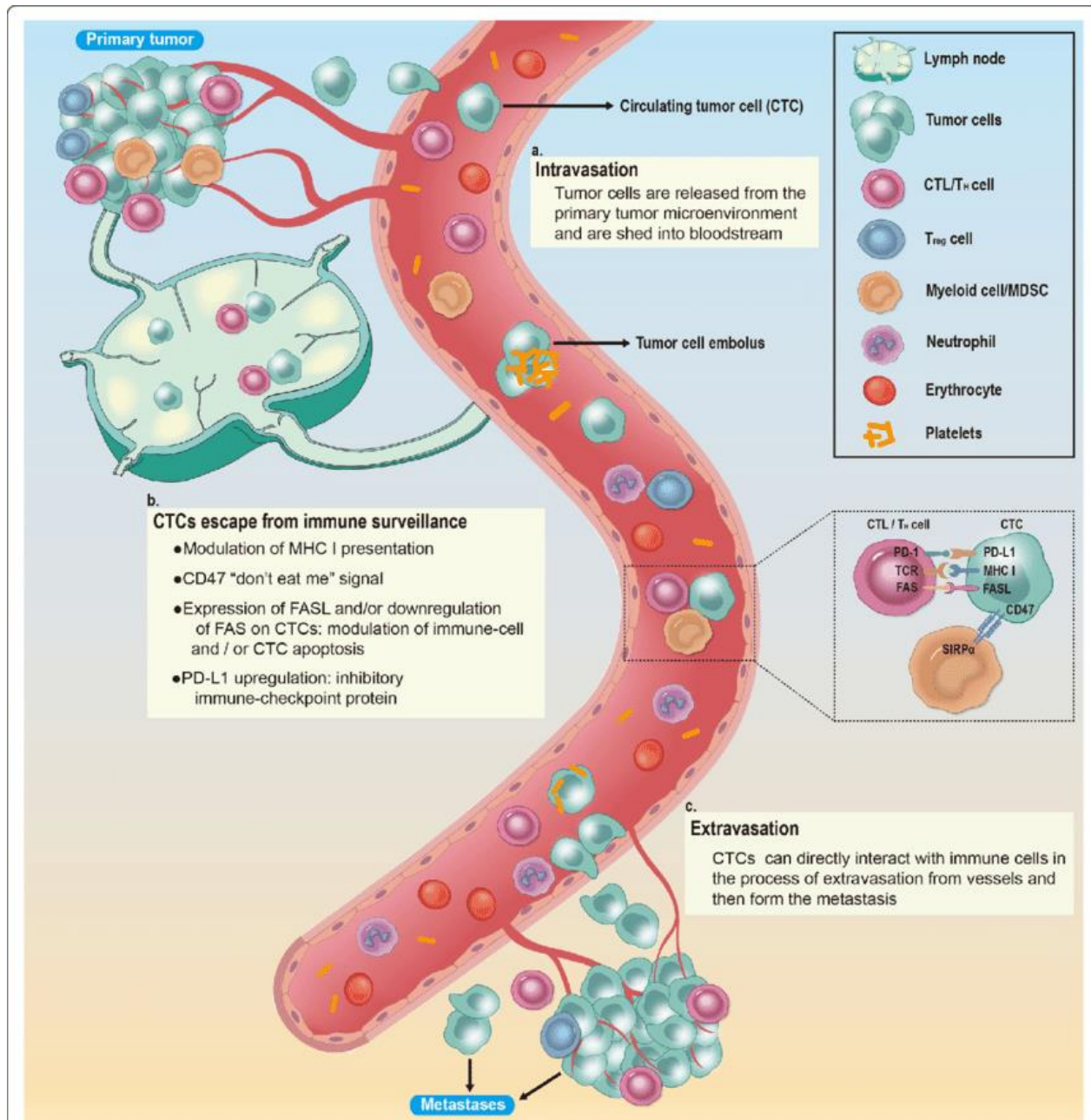


Figure 1 Represent different steps in cancer metastasis Three main process i.e., Intravasation (Released of tumor form its primary site and intravasate blood stream), Escape form immune surveillence and finally extravasation of tumor cells to other sites (Zhong et al., 2020).

2.2 Protein kinase C

Protein kinase c (PKC), a serine/threonine specific kinase, is family of proteins unlike other Protein kinases activated independent of cyclic nucleotide with dynamic functions ranging from cell signaling, proliferation, differentiation, and memory to carcinogenesis (Takai, Kishimoto, Inoue, & Nishizuka, 1977) (Murray, Baumgardner, Burns, & Fields, 1993) (Ashendel, 1985) (Alkon, 1989) (Cutler Jr et al., 1993). To date 10 isoforms of PKC has been discovered that are categorized into three different categories i.e., conventional PKC (cPKC), novel PKC (nPKC) and atypical PKC (aPKC) and this division is based on the process of their activation and the required cofactors. Ca^{2+} and DAG is required for the activation of cPKC, while aPKC does not required Ca^{2+} and DAG, and the activation of nPKC DAG but not Ca^{2+} . PKC proteins contain four conserved regions separated by five variable regions with lower homology among them. The regulatory and catalytic domains are present at N-terminus and C-terminus respectively. A common phosphatidylserine (PS) binding domain is present in all isoforms of PKC which enable them to interact with plasma membrane after their activation and translocation from the cytosol (Webb, Hirst, & Giembycz, 2000).

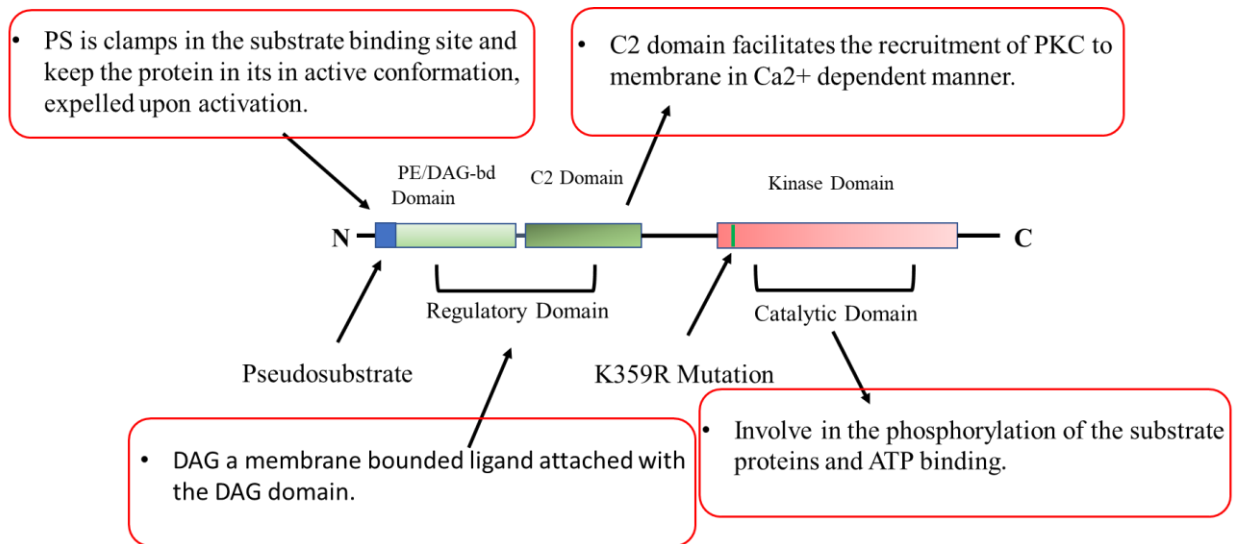


Figure 2 Schematic diagram of PKC gamma representing different domains of the protein i.e., PE/DAG domain, C2 domain and kinase domain and their functions.

2.3 Maturation

The PKCs required two steps to be fully functional. First their maturation and priming and second their activation. The maturation of PKCs involved phosphorylation, at different site which stabilized their catalytic domain, along with mammalian target of rapamycin complex 2 (mTORC2) and heat shock protein-90 (HSP90) required for priming and maturation of PKCs (Parker & Parkinson, 2001) (Gould, Kannan, Taylor, & Newton, 2009; Guertin et al., 2006). The interaction/binding of HSP90 and Cdc37 to the kinase domain of the cPKC and nPKC was suggested to be the initiative step in their maturation (Gould et al., 2009) and alteration in this mechanism was identified to be involved in different diseases i.e. cancer (Akamine et al., 2003).

2.4 Activation

The activation of cPKCs involved four different interactions and the translocation of PKCs from cytosol to the plasma membrane where they are attached with the specific binding

domain. The four basic interactions are Ca^{2+} dependent interaction of inactive PKC isoform with membrane, association of C1 and C2 domain with membrane at two distinct site, PKC conformational change via membrane interaction and DAG/phorbol diester dependent conformational changes in membrane bound PKCs (Webb et al., 2000). The activity of PKC is compartmental, RACK an anchorage protein, annexins and other cytoskeletal proteins' dependent (Mochly-Rosen, 1995). The association/penetration into the cell membrane of PKC (cPKC & nPKC) and their activation is DAG dependent (Bell & Burns, 1991; Lester, Doll, Brumfeld, & Miller, 1990).

2.5 Role of Ca^{2+} and fatty acid

Intracellular level of Ca^{2+} and phosphatidylserine (PS) are crucial regarding cPKCs activation. The elevation in Ca^{2+} upon stimulation of the receptor and mobilization of Ca^{2+} to sufficient level has very critical role in the translocation of cPKCs and subsequently their activation (Zidovetzki & Lester, 1992). The electrostatic attachment of PS as cofactor to the Pseudosubstrate binding site in PKC play important role in PKC activation and hydrophobic interaction with membrane is also required to counter the impact of unsaturated fatty acid chain length in DAG and PS (Brumfeld & Lester, 1990; Lapetina, Reep, Ganong, & Bell, 1985; Mosior & McLaughlin, 1991).

2.6 Protein Kinase C Gamma

Protein kinase C gamma isoform is an enzyme belongs to the large family of PKC proteins, a serine-threonine specific protein kinases, encoded by *PRKCG* gene located on chromosome 19 at position 19q13.2-q13.4. (L. Coussens et al., 1986), (Johnson et al., 1988). During the course of different studies scientists have find out that activation of protein kinase

C depends on calcium ions along with diacylglycerol (DAG) rather than cyclic nucleotides unlike other protein kinases thus named as Protein kinase C and later on different isoforms of this proteins have been identified (L. Coussens et al., 1986; Y. Takai et al., 1979; Takai, Kishimoto, Kikkawa, Mori, & Nishizuka, 1979). PRKCG protein is 697 amino acid long contain 18 exons (Asai et al., 2009). The structural alignment of PKC alpha, PKC beta and PKC gamma revealed that PRKCG has 4 conserved domains involved in regulatory and catalytic activities and 5 variable regions. The conserved domains are preserved in all the three isoforms of PKC, but comparatively PKC gamma is more variable from the remaining two (Adachi et al., 2008), (L. Coussens et al., 1986). The expression of PRKCG protein has been identified in various organs but is most abundant in brain and spinal cord and especially the hippocampus cerebral cortex and cerebellum (Saito & Shirai, 2002). The phosphorylation of DAG kinase gamma ($DGK\gamma$) at Ser-776 and Ser-779 by PKC gamma at AD domain in the presence of Ca^{2+} and phosphatidylserine (PS) activate and translocate $DGK\gamma$. The activated $DGK\gamma$ in turn metabolized Diacylglycerol (DAG) to phosphatidic acid and act as negative regulator of $PKC\gamma$. Both PKC gamma and DAG kinase gamma translocate to the membrane after their activation, but the activation of DAG kinase gamma is $PKC\gamma$ dependent. The overall process shows the regulated activation and expression of both $PKC\gamma$ and $DGK\gamma$ (Yamaguchi et al., 2006). In the context of gap junction assembly/disassembly the PKC gamma was found to positively regulated by Lens epithelium-derived growth factor (LEDGF). The analysis of protein-protein interaction reveals the phosphorylation of Connexin 43 by PKC gamma was enhanced and in turn decrease the activity of gap junction and plaques of gap junction (Nguyen, Boyle, Wagner, Shinohara, & Takemoto, 2003).

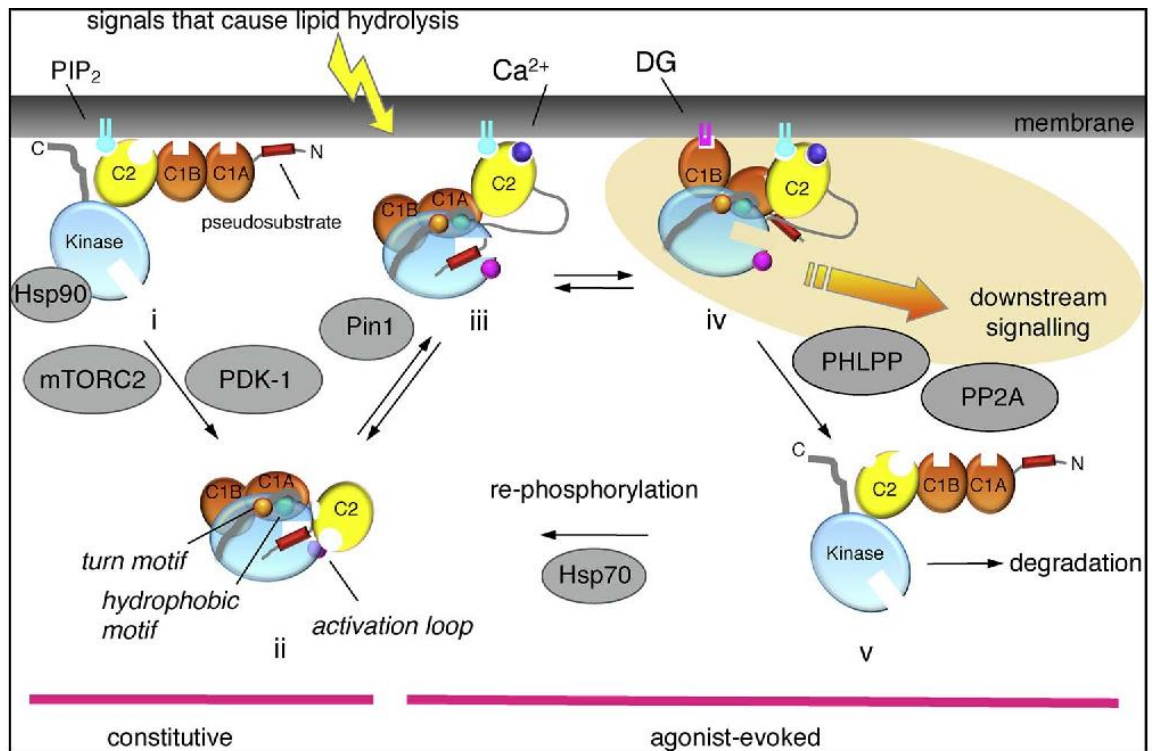


Figure 3 Diagrammatic representation of cPKC maturation and activation. (i) Shows newly synthesized protein with exposed Pseudosubstrate site at N-terminal, (ii) Hsp90 dependent phosphorylation of kinase domain via mTORC2/PDK-1 (iii) Ca^{2+} dependent translocation to plasma membrane (iv) binding of protein with DAG and downstream signaling (v) re-phosphorylation of protein to sustain its signaling lifetime (A. C. Newton, 2018).

2.7 Role of PKC gamma in cancer

The role of PKC gamma in the development and progression is well established. Several studies determined that the PKC gamma is associated with cancer at different stages i.e., glioma, kidney cancer, colon cancer and liver cancer etc. However, all those studies established the role of PKC gamma progression, development, its differential expression in various cancers but these studies do not provide sufficient information about the role of genetic polymorphism and its association with carcinogenesis. PKC gamma a member of PKC family located on chromosome 19 at position 19q13.2-q13.4. The activation of PKC gamma depends on calcium and diacylglycerol (DAG) (Lisa Coussens et al., 1986).

Several studies on PKC proteins has established their role in regulation of cell growth, proliferation, differentiation, migration and apoptosis etc. (A. R. Black & Black, 2012). The role of PKC gamma has been implicated in many cancer types i.e. glioma, colon cancer, osteosarcoma etc. but there was found to be differential expression of PKC gamma not only in cancer type but also in different cell lines (SW480, Lovo, HT29, Coco2 and IEC-18) of the same cancer type (colon cancer), which also confer the role of PRKCG in the colon cancer (Garczarczyk, Szeker, Galfi, Csordas, & Hofmann, 2010). Another study also indicates the role of PKC gamma in colon cancer, which revealed the up-regulation of PKC gamma in almost half of the sample implicating its role in tumor development and the experiment was validated by the inhibition of the gene via siRNA which remarkably reduce cell migration and thus tumorigenesis (Dowling et al., 2017). A study of mouse xenograft models identified the role of fascin, an actin-bundling protein, in migration and tumorigenesis in different cancers. It also determined the role of Rac1 as the regulator of PKC gamma and fascin interaction in the colon cancer and were found to be over expressed and colocalized in the cancerous cells. Phosphorylation of Fascin, active Fascin and PKC gamma are three major contributors in this whole phenomenon. Furthermore, the study also ruled out the role of cdc42 as Fascin and PKC gamma's regulator (Parsons & Adams, 2008). The phosphorylation of Myosin IIB by PKC gamma upon activation by EGF shows that over expression of PKC gamma can lead to aberrant phosphorylation and cell motility and may involve in prostate cancer (Rosenberg & Ravid, 2006). The analysis of paraneoplastic cerebellar degeneration (PCD) and non-small cell lung cancer (NSCLC) has determined the role of PKC gamma in NSCLC. The study identified that there may be a correlation between the PCD and PKC gamma expressed in tumor cells (Sabater et al., 2006). One of the

comparative genomic study shows the increased copy number of PKC gamma as well as some other isotypes of PKC genes in ovarian cancer which implicates the potential role of the PKC gamma in tumor (L. Zhang et al., 2006). The differential protein expression of Conventional PKC (cPKCs) exhibits the role of these proteins and their expression in gastric cancer and multiple drug resistance (MDR). The protein analysis shows an up-regulation of PKC gamma in gastric cell line SGC7901 as well in the SGC7901/VCR a drug resistance cell sublines but there was no remarkable difference in the expression profile of PKC gamma, but still it determined its role in the development of gastric cancer (Han et al., 2002). PKC gamma overexpression was also found to play a significant role in ER-negative breast cancer and PKC gamma transfected immortalized murine mammary epithelial cells (NMuMG), as it shows with PKC gamma shows high rate colony formation, epithelial-mesenchymal transition (EMT) via up-regulation fibronectin, integrin and down-regulation of E-cadherin and motility, etc. which are the hallmarks of tumorigenesis (Mazzoni, Adam, de Kier Joffe, & Aguirre-Ghiso, 2003), (Morse-Gaudio, Connolly, & Rose, 1998). The regulation and translocation of Heat shock protein (Hsp90 α) is mediated by PKC gamma and PLC signaling and was found to bind with the vesicle present on the cell surface of tumor cells and play key role in tumor invasion. As the Hsp90 α is regulated by PKC gamma, the overexpression of it can mediate cell motility, invasion and metastasis (Yang et al., 2014). Genetic analysis of PKC gamma presents that single nucleotide polymorphisms (SNPs) may involve in osteosarcoma either as a susceptibility factor as a causative agent. PKC gamma variants i.e. rs454006 and rs454006, identified to have different allele frequency and were significant between patients and healthy individuals, with implicates that there is the potential role of PKC gamma polymorphism in osteosarcoma development

and tumorigenesis (Y. Zhang et al., 2014), (Lu et al., 2015). The glioma cell line (U-251 MG) were transfected with PKC gamma and PKC δ and up-regulates their expression in U-251 MG, but the overexpression of these protein exert contradictory effect on the cells as PKC gamma overexpression induced by epidermal growth factor (EGF) elevate DNA synthesis, proliferation and invasiveness, interestingly there was one other study which implicates that the overexpression PKC gamma in different cell lines of glioma U87 and U251 reduced proliferation, cell motility, invasion and shows suppressive effect on glioma, so this opposing role of PKC gamma in different glioma cell lines maybe due to some cell milieu which needs to further sort out (Mishima, Ohno, Shitara, Yamaoka, & Suzuki, 1994), (Finniss et al., 2006). The examination of neuroblastoma samples and their cell lines established the role of cPKCs i.e., PKC α , β and PKC gamma. The up-regulation of these proteins increased growth rate and proliferation of the tumor cell, but when inhibited a significant decline in proliferation and increased apoptosis was observed which validates the role of cPKCs in neuroblastoma development and survival (Zeidman et al., 1999). Investigation of B-cell lymphoma suggested that PKC gamma can be used as prognostic marker (Kamimura, Hojo, & Abe, 2004).

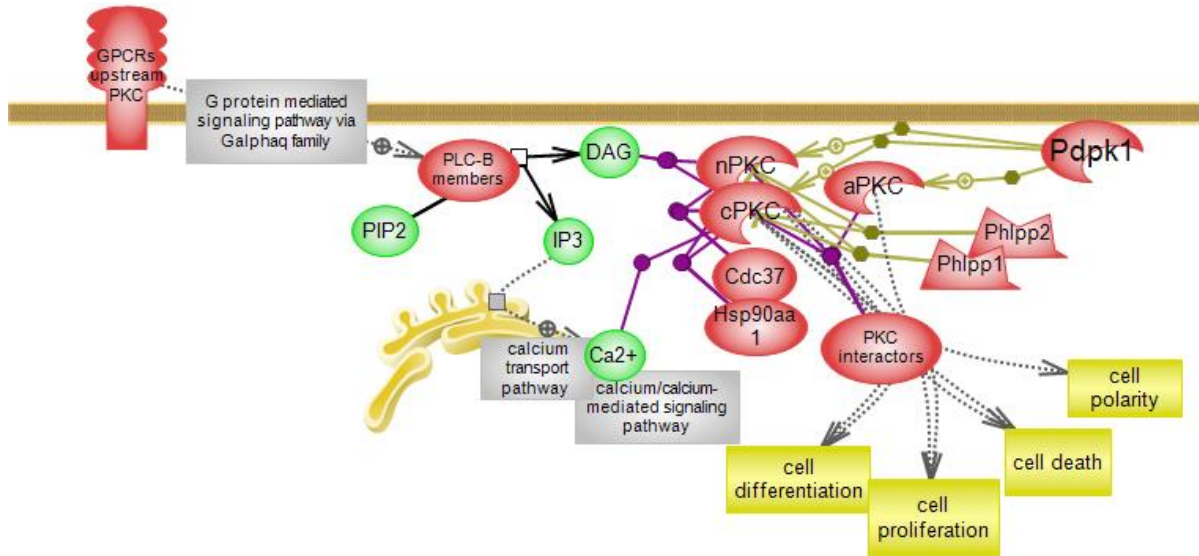


Figure 4 Schematic diagram of PKC signaling shows the role of cPKC and nPKC in different types of cell processes i.e., Cell proliferation, differentiation, apoptosis and cell polarity, etc (Gallegos & Newton, 2008).

2.8 PKC gamma signaling

Conventional PKCs signaling pathways and their activation is almost the same, but their expression level is different in different tissues and sometimes play contradictory role in different cell lines. Just like other cPKCs, PKC gamma is activated by DAG and calcium ions downstream of receptor tyrosine kinases (EGFR, PDGFR), which is activated upon ligand (growth factor) binding and become dimerized and in turn activates phospholipase c (PLC) (M. R. Smith, DeGudicibus, & Stacey, 1986), (Margolis et al., 1989). Subsequently the dimerization of receptor tyrosine kinase (RTK) also creates binding site for phosphoinositide 3-kinase (PI3k) due to auto phosphorylation of its tyrosine residues in cytoplasmic domain (Vivanco & Sawyers, 2002), which then hydrolyzed phosphatidylinositols (PtdIns) and generation of DAG and inositol phosphates (IPs). After

that IPs induced release of Calcium ions, activation and translocation of cPKC from cytosol to plasma membrane and activation and secretion of Hsp90 α occurs (Wang et al., 2012), (Nishizuka, 1992; Peters et al., 1992).

2.9 PKC gamma and its interacting partners

Several studies have shown the regulation of growth rate, invasion, metastasis and metabolism, thus controlling tumor development via AMP-activated protein kinase (AMPK) activity (Shackelford & Shaw, 2009). Another study demonstrated the negative regulation of PKC via the activation of AMPK which inhibit its function (Kong, Liu, Yu, Lu, & Zang, 2012). The inhibition of Hsp90 α via the activation AMPK α 1 by metformin and one other studies revealed that only PKC gamma is involved in the phosphorylation and translocation of Hsp90 α across the membrane which mediates tumorigenesis and metastasis (Yang et al., 2014). One other study shows that tissue plasminogen activator (tPA) induced activation of PKC gamma can leads to Raf-MEK pathway signaling transduction, without the involvement of Ras protein, thus leads to cell proliferation and differentiation (Takahashi, Ueno, & Shibuya, 1999). The inhibition of Δ Np63 α a positive regulator of miR-320a reduced the level of miR-320a and in turn up-regulate PKC gamma and elevated phosphorylation of Rac1 at Ser71, leading to increased proliferation and invasion, which confirm the role of PKC gamma role in cell cycle regulation and its upstream regulators and it also suggest the interaction of PKC gamma and Rac1 (Aljagthmi et al., 2019). Another study shows the negative correlation of PKC gamma with expression level of transthyretin and also determined that ethanol treatment can reversed the expression of transthyretin and down-regulate the protein in PKC gamma null mutant mice but have no effect on wild type (A. M. Smith, Bowers, Radcliffe, & Wehner, 2006). The role of PKC gamma has also been

established in the differentiation of 3T3-L1 and 3T3-F442A adipocytes. The expression of PKC gamma was found to be elevated during the process of differentiation but reduced in the mature adipocytes (FLEMING et al., 1998). PKC gamma and PKC ϵ both are activated during oxidative stress and were found to have interaction with gap junction protein connexin 43 (Cx43) in heart and neural tissue and also protect these tissue from ischemia (Barnett, Madgwick, & Takemoto, 2007).

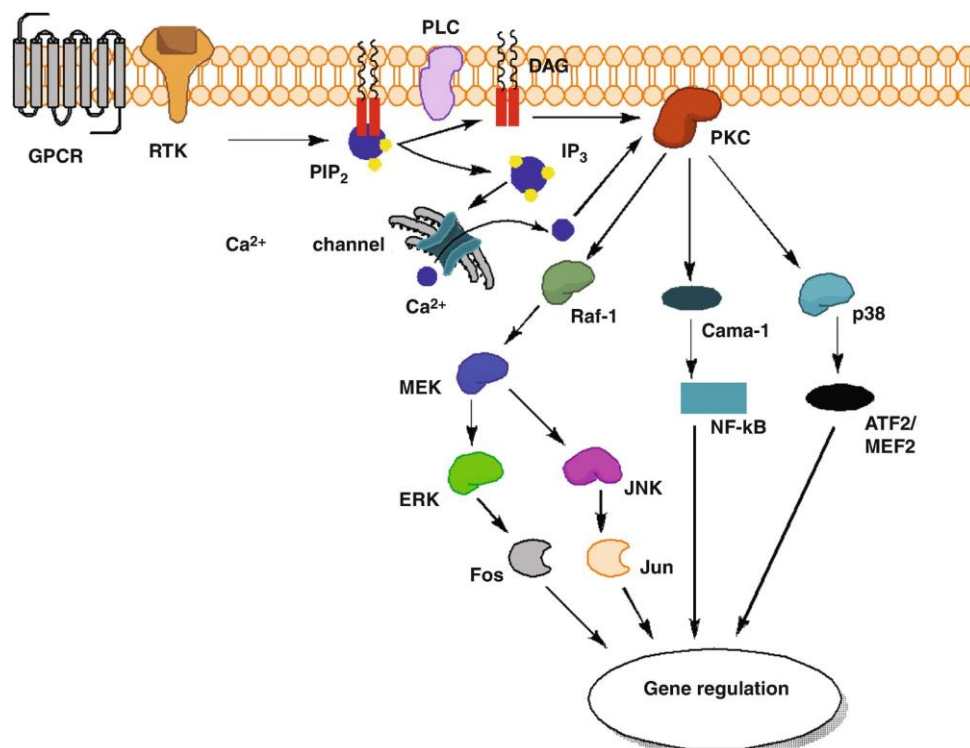


Figure 5 Shows the schematic representation of PKC signaling, its interaction partners i.e., proteins of MAPK pathway, NF-K β beta pathway, etc. and its role in gene regulation (Adrian R Black & Black, 2013).

2.10 PKC gamma inhibitors

Considering the role of PKC gamma in cancer, scientist searched for compounds that can inhibit PKC activity and are also specific to isozymes. Different approaches were used in

the development of inhibitors based the target site i.e., C1 domain, ATP binding site and RACK interactive regulatory region, etc. some of those drugs are listed in Table 1.

2.10.1 Enzastaurin

Enzastaurin (LY317615.HCl) a potent inhibitor of PKC and was found to inhibit the activity of PKC by binding to its ATP binding domain as both ATP and Enzastaurin compete for the same site and act as inhibitor of multiple myeloma (MM). It was also determined that Enzastaurin can also inhibit the phosphorylation of PKC at Thr-514 and blocked the release of active PKC from the plasma membrane to the cytoplasm and in turn the inhibition of molecules downstream of the PKC. The half maximal inhibitory concentration IC_{50} of Enzastaurin for PKC gamma is 83 nM and the drug is still in phase 2 clinical trials (Podar et al., 2007).

2.10.2 Staurosporine

Staurosporine another inhibitor of the PKC which was found to interaction the Ca^{2+} binding domain of PKC and block the site. This blocking results in the inhibition of PKC activity as Ca^{2+} is required for the activation PKC. The required IC_{50} of staurosporine was determined to be 32 nM (Wilkinson, Parker, & Nixon, 1993).

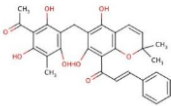
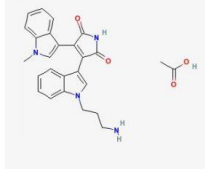
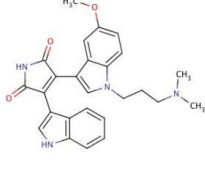
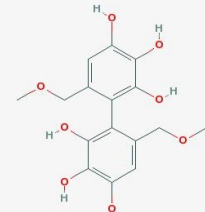
2.10.3 Bisindolylmaleimides

Drugs belong to bisindolylmaleimides i.e., Ro 31-8220, Ro 31-8425, Ro 31-8425, and Ro 32-0432 also act in the similar manner as staurosporine does. These drugs also interact with the cation-binding site and as result block the binding of calcium ion needed for PKC activation. The IC_{50} of Ro 31-8220, Ro 31-8425, Ro 31-8425 and Ro 32-0432 for PKC gamma inhibition is 27 nM, 13 nM and 37 nM respectively (Wilkinson et al., 1993).

2.10.4 Midostaurin

Midostaurin (PKC412; CGP 41251) is derived from the previously identified PKC inhibitor, staurosporine and act as broad spectrum anticancer and antiproliferative agent. The IC_{50} required for PKC inhibition is 24 nM and the drug is in clinical trials and in different phases in various pharmaceutical companies (Fabbro et al., 2000).

Table 1 shows different PKC inhibitors, their structures, mechanism of action, half maximal inhibitory concentration (CI_{50}) along with the references.

Drugs	Structures	Mechanism of Action	CI_{50}	References
Rottlerin		Apoptosis and autophagy via a PKC δ -independent pathway	5.3 μ M	(Gschwendt et al., 1994)
Bisindolyl maleimide VIII		DR5-mediated apoptosis through the MKK4/JNK/p38 kinase	195 μ M	(Zhou et al., 1999)
Gouml 6983		Ca $^{2+}$ mediated inhibition of PKC	6 nM	(Young, Balin, & Weis, 2005)
HBDDE		Caspase-3 induced apoptosis	50 μ M	(Kashiwada et al., 1994)

Chapter 3 Methodology

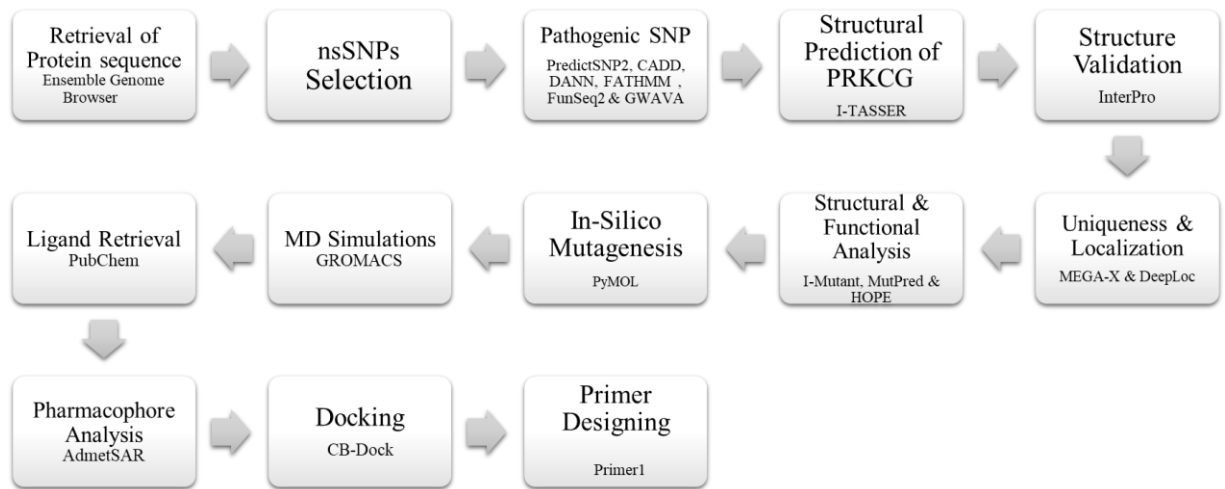


Figure 6 Flow chart of different in-silico methods that were followed in this study.

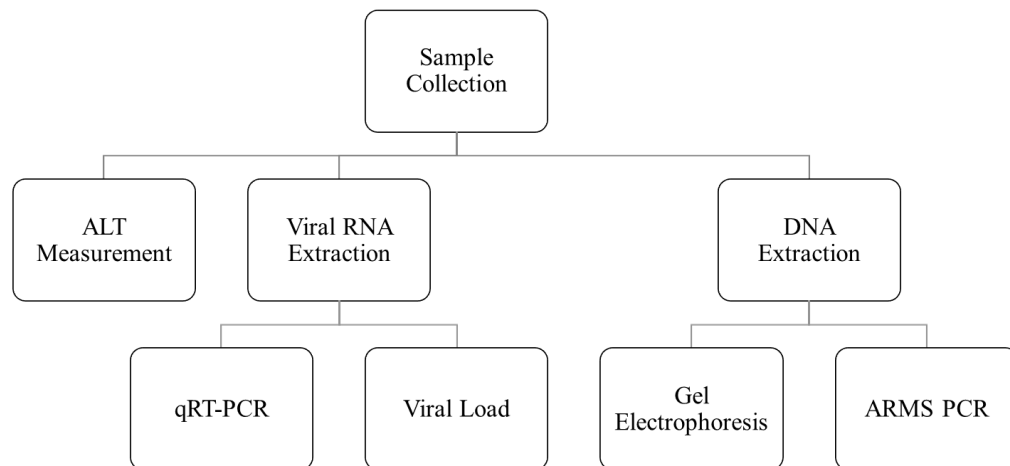


Figure 7 Workflow of In-vitro methodology.

3.1 Structure Prediction of PKC gamma

The amino acid sequence of the protein PKC gamma was submitted to I-TASSER (Roy, Kucukural, & Zhang, 2010) for structure remodeling and prediction. After that I-TASSER predict five models for the target protein. From results page model 3 was selected for further analysis.

The protein amino acid sequence in FASTA format was used as input in InterPro (Blum et al., 2021) for computational validation and prediction of the protein family and the domains that are present in the it.

3.2 Uniqueness and Localization

To predict the localization of the PKC gamma the amino acid sequence of the protein was submitted to a web-based tool known as DeepLoc to analysis where exactly the protein is compartmentalized in the cell, while for uniqueness the amino acid sequences of all the members of PKC family were retrieved and then submitted to a software MEGA-X to predict the phylogenetic tree of the protein and its uniqueness.

3.3 Retrieval & Identification of Pathogenic SNPs

The Ensemble Genome browser was accessed on 15th November 2020. In search bar human and PRKCG was typed and used as input. The SNPs present in the gene were located from variant table and only missense SNPs were selected as per our study requirement and 429 missense SNPs was provided by Ensemble. Fig.3 shows graphical representation of SNPs retrieval from Ensemble Genome Browser. These missense SNPs were then subjected to different tools i.e, PredictSNP2 (Bendl et al., 2016), CADD (Rentzsch, Witten, Cooper, Shendure, & Kircher, 2019), DANN (Quang, Chen, & Xie, 2015), FATHMM (Shihab et al., 2014), FunSeq2 (Fu et al., 2014) and (Ritchie, Dunham, Zeggini, & Flicek, 2014) listed in

table 2, to analyze the high-risk SNPs among the 405 SNPs retrieved from Ensemble genome browser.

Table 1 List of different computational tools that were used to predict pathogenicity of nsSNP, their scoring criteria and classification.

Tools	Score Range	Classification	
		Neutral	Deleterious
PredictSNP2	0-1	<0.5	>0.5
CADD	1-99	<20	>20
DANN	0-1	<0.5	>0.5
FATHMM	0-1	<0.5	>0.5
FunSeq2	0-1	<0.5	>0.5
GWAVA	0-1	<0.5	>0.5

3.4 Structural and Functional Analysis

To analysis the structural and functional impact of residual change on protein, an in-silico tool, HOPE (Venselaar, Te Beek, Kuipers, Hekkelman, & Vriend, 2010) was used. Amico acid sequence of protein kinase C gamma was used as input. Substitution and amnio acid positions were selected in the subsequent steps. A comprehensive report was generated at the end provides information regarding impact of amnio acid change on protein structure and hence its function. Two other computational tools I-Mutant (Capriotti, Fariselli, &

Casadio, 2005) and MutPred (Pejaver et al., 2017) were also used to predict the impact of amino acid change on protein structure and function.

3.5 Molecular Dynamic Simulations

The molecular dynamic simulation for both wild type and mutated protein was carried out via GROMACS software (Bekker et al., 1993), through which supercomputer was accessed. Feeding of data to supercomputer PuTTY was used and for file transfer between supercomputer and PC was conducted through WinSCP and SFTP file transfer protocol was used. The was to find out the impact of missense mutation in PKC gamma protein on protein structure in. So, 20 nanoseconds simulation was run for both wild and mutated protein and then analyzed different parameters i.e., Root mean square deviation (RMSD), Root mean square fluctuation (RMSF), Radius of gyration and number of hydrogen bonds for comparison.

3.6 Protein Docking

Protein-ligand docking was performed using CB-Dock (Y. Liu et al., 2020). I-TASSER predicted protein structure in PDB format was used as receptor input file and Maytansine as ligand in SDF format and the parameters were kept as default. CB-Dock predict five possible protein-ligand interactions based on vina score and cavity sized. The interaction with lowest energy was selected as it was predicted to be the stable interaction among the five given by CB-Dock. To interpret the protein-ligand binding at molecular level LigPlot+ (Wallace, Laskowski, Thornton, & selection, 1995) was used. The predicted protein-ligand structure from CB-Dock was used as input. LigPlot+ showed the protein cavity to which the ligand was bind and chemical bonds i.e., hydrogen bond and hydrophobic interaction between amino acids and ligand. LigPlot+ give the 2D demonstration of protein-ligand interaction

and 3D format was visualized via PyMOL. For ligand PubChem (Kim et al., 2021) database was accessed. In search bar Maytansine was typed and then 2d structure in SDF format was downloaded. To study the properties of the Maytansine its SMILES was copied from PubChem and searched in AdmetSAR (Cheng et al., 2012) an online website which provide ADMET (Absorption, Distribution, Metabolism, Excretion and Toxicity) properties.

3.7 Primer Designing

The PCR primers were designed computationally via Primer1 (A. Collins & Ke, 2012; A. C. J. C. r. Newton, 2001) used for tetra ARMS PCR. The genome sequence mapped from chromosomal assembly 38.p13. was used as input in the Primer1. SNP position and allele difference was selected, and the remaining option were kept as default.

3.8 Genomic DNA Extraction

The blood samples were collected in EDTA tubes. From each sample 750µl of blood along with 750µl of solution A was taken using 1000µl pipette in eppendorf tubes. The tubes were kept at room temperature for 10 minutes and then centrifuged at 13000 rpm for 1 minute. This step was repeated twice as solution A contain lysis buffer so the membrane should lyse properly. After that supernatant was discarded and the pellet was resuspended in 400µl of solution B, dissolved properly and centrifuged again at 13000 rpm for 1 minute. The supernatant was discarded after centrifugation and the nuclear pellet was again resuspended in 400µl of solution and 12µl of 30% SDS and 5µl of proteinase k was added as well. The samples were kept overnight at 37°C in an incubator.

The samples were taken out from the incubator and 250 μ l of solution C and 250 μ l was added and then centrifuged for 13000 rpm for 10 minutes. The upper aqueous layer having DNA was transfer carefully to a new eppendorf tube with picking any particles from the lower layer containing protein and cell debris. After that 55 μ l of 3M sodium acetate and 500 μ l of ice chilled isopropanol was added to the sample and then inverted several times so the DNA can be precipitated. The sample was again centrifuged at 13000 rpm for 10 minutes. The supernatant was discarded, and DNA was resuspended in 200 μ l of 100% chilled ethanol and centrifuged again at 13000 rpm for 8 minutes. The ethanol was then removed from the tube and let the sample air dry so that ethanol can be completely evaporated. The DNA was then diluted in 200 μ l of TE buffer or PCR water.

3.9 Polymerase Chain Reaction

Tetra amplification-refractory mutation system polymerase chain reaction (ARMS PCR) was used for the detection of point mutations in the DNA extracted from blood samples. Two sets of primers two outer and two inner primers (Outer forward and reverse) and (Inner forward and reverse). The purpose of the outer primers was to amplify the whole gene and to detect the SNP inner primers were used which was allele specific. 25 μ l of PCR reaction was prepared with 9.5 μ l of Solis BioDyne® master mix, 1 μ l of all the four primers and 10.5 μ l of water. The annealing temperature was optimized at 60°C. The PCR samples were then sort spined to mix all the entities properly. After that Gradient PCR machine was used to

carry out samples at multiple temperature simultaneously, as each row has different temperature. A total of 35 cycles was run which takes approximately 1.5-2 hours.

3.10 PCR Steps and Conditions:

Step 1: In first of PCR all the DNA molecules are denatured, and the hydrogen bonds breaks between the strands. Initially the denaturation of DNA was performed at 95°C for 5 minutes which completely melt the DNA. This step was not repeated in stage two, instead DNA denaturation occurred at 94°C for 30 seconds and having 35 cycles.

Step 2: The annealing of DNA occurs in this step as gradient PCR was used so multiple temperatures were set and this step took 30 seconds too.

Step 3: Polymerization of the DNA occurred right after annealing step at 72°C for 30 seconds and finally the DNA was polymerized for 7 minutes at 72°C.

3.11 PCR Mixture Preparation

PCR was performed in a single tube containing 25 µl of reaction volume made up of Solis BioDyne® master mix (9.5µl), Forward outer/inner and Reverse outer/inner (1 µl each), template DNA (1µl) and ddH₂O (10.5µl).

3.12 Gel Electrophoresis

Gel electrophoresis is a molecular biology technique used to separate DNA fragments according to their size. The technique involves the loading of DNA samples into the wells

in gel and applying the current. As the DNA is negatively charged molecule that's why it will migrate towards the positive electrode and thus DNA fragments of different sizes will be separated as the electrophoretic mobility of each fragment will be different. The DNA fragments can be seen as band in gel visualized under UV light.

3.13 Agarose gel preparation

Weigh 1 or 2g of agarose powder on digital balance depending on the product to be run on gel. Add agarose powder into flask along with 100mL of 1xTAE. Microwave for 3minutes until the agarose is completely dissolved and the solution become transparent and after that allow it to cool down at room temperature. Add 3-5 μ l of Ethidium-Bromide (EtBr) to agarose. Pour the agarose into a gel tray and place the comb in the gel. The gel is allowed to solidify at room temperature for 20-30 minutes. The comb was removed after the gel was solidified. The gel tray was placed in tank and the gel was immersed in buffer (1x TAE) inside the tank.

3.14 ALT/SGPT Test

An Alanine aminotransferase (ALT) test was performed for both patients and control samples to diagnose the effect of vial induced HCC on liver. A kit-based method was used for this purpose. Blood samples of both patients and control were collected in empty tubes and not anticoagulating was added. After a few minutes the blood clot and then centrifuged at 3000rpm for 2 minutes to extract serum which contain ALT enzymes. The kit contains two reagents R1 (Alanine tris buffer) and R2 (Alpha keto glutamate). Both the reagents were added in 4:1, 400 μ l of R1 and 100 μ l of R2 was taken in separate tube and 50 μ l of sample was then added to it, required no incubation period. The ALT concentration was checked using Microlab 300 semi-automated spectrophotometer at 340nm.

3.15 Viral RNA Extraction

To analyze the viral load in patient sample, viral RNA was extracted from the blood via FAVOREGEN KIT[®]. 200 µl of blood was taken in an eppendorf tube and 500 µl of VEN buffer was added and vortexed for 5-7 seconds. After vortexing 500 µl of 75% ethanol was added to the tube and again vortexed for 5-7 seconds. In the next step spin column was used. The sample from the eppendorf was transferred to spin column and centrifuged at 8000rpm for 1 minute. The collecting tube was discarded, and the filter tube was aging put in a new tube. 500 µl of wash buffer 1 was then added and again centrifuged at 8000 rpm for 1 minute. The collecting tube was changed and 750 µl of wash buffer 2 was added and centrifuged at 14000rpm for 1 minute. This step was repeated twice so the filter gets dried. Filter tube was transferred to eppendorf tube and 50 µl of RNAase free water was added at the end and centrifuged again at 8000rpm for 1 minute. The RNA in the sample was transferred from filter to the tube and kept at -20°C.

3.16 Quantitative Reverse Transcriptase Polymerase Chain Reaction (qRT-PCR)

qRT-PCR was used to simultaneously quantify and amplify viral RNA. Reverse transcriptase enzyme is used to convert viral RNA into DNA. The quantity is determined by intensity of the fluorescent, so for this purpose SYBR green dye was used which attached with the minor groove of the dsDNA but does not bind with ssDNA. Over time the fluorescence changes and is recorded against the cycles and a plot is generated which shows the amplification progress of the PCR. For sample preparation 6 µl of each sample, 43 µl of master mix and 1.2 µl of reverse transcriptase enzyme is mixed in a single PCR tube. Two standards of known

concentration one lower and one upper limit was used to determine the viral load of the samples. A liner plot is generated after the viral concentration is compared with standard curve which provides the starting quantity the template molecule on x-axis against the cycle threshold (CT) on Y-axis. The sample with higher starting quantity/copy number will have sample CT value compared to sample with smaller copy number.

Chapter 4 Results

4.1 Structure of PKC Gamma

The 3-dimensional structure of PKC gamma was predicted via I-TASSER which is the most advance and reliable tool which predict protein structure based on multiple threading approach. I-TASSER predicted 5 different models. Among the five models' model 3 was selected based on the C-score (-2.53) and protein folding and was then visualized through PyMol. The Protein structure was computationally validated via InterPro, an online tool, by categorizing proteins in families and predicted different domains in the proteins. InterPro predicted four domains in the PKC gamma protein i.e. PE/DAG-bd Domain, C2 Domain, Prot_kinase Domain and AGC_kinase C Domain and are shown in red, blue, yellow and magentas color respectively. Fig 1 represent PRKCG model predicted by I-TASSER

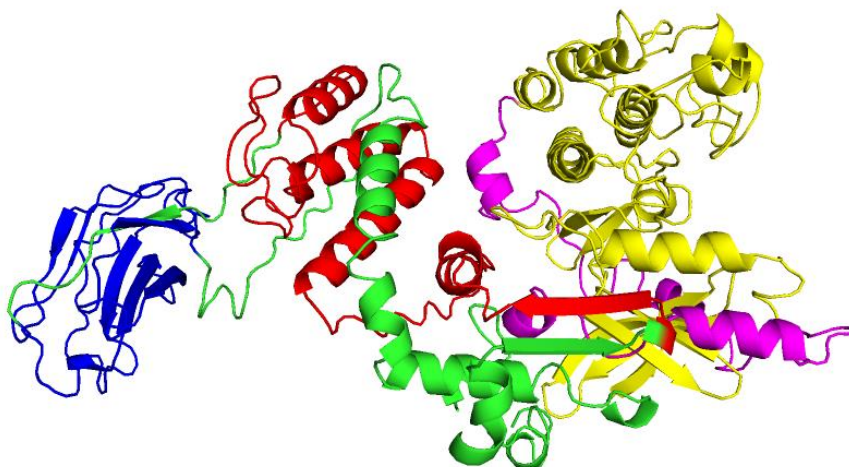


Figure 8 Represent model 3 of PKC gamma predicted via I-TASSER with C-score (-0.53). The protein structure is colored in green, and domains are highlighted in different colors. DAG domain (red color), C2 domain (blue), kinase domain (yellow) and AGC kinase (magenta).

4.2 Phylogenetic Tree and Subcellular Localization

The route of PKC gamma localization is given in figure 9. The red line represents the path taken by the protein to localize to its compartment within the cell. The score shows the probability/likelihood of the event. So, it is suggested based on the score that PKC gamma is localized in the cytoplasm. The phylogenetic profile of the PKCs is shown in figure 10 which shows that all the members of PKC gamma are originated from a common ancestor protein. The score represents the substitution per site, mean that how much a particular protein evolve with the time from its other family members.

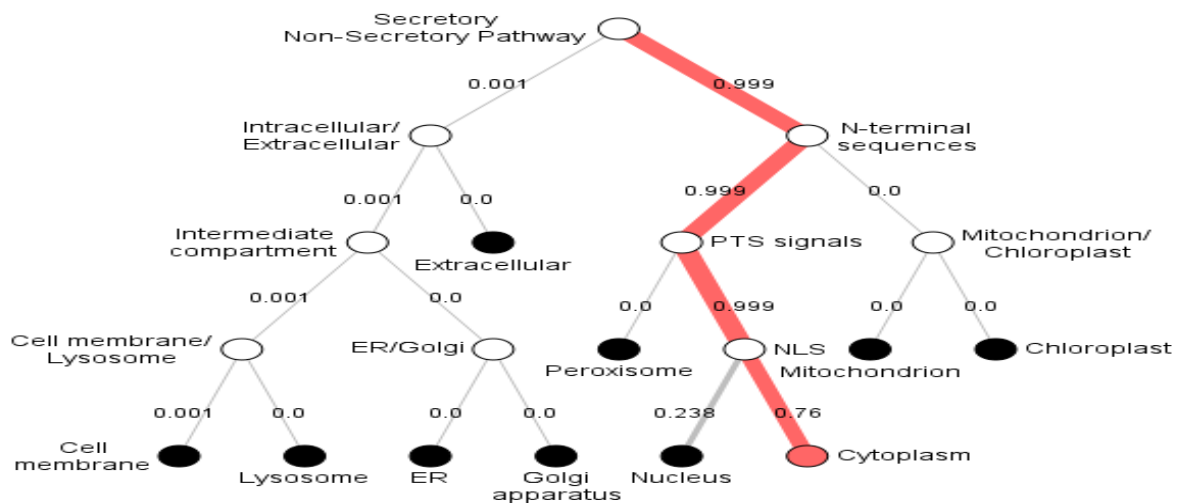


Figure 9 Localization route of the PKC gamma protein along with the probability score. The red line shows the path of localization.

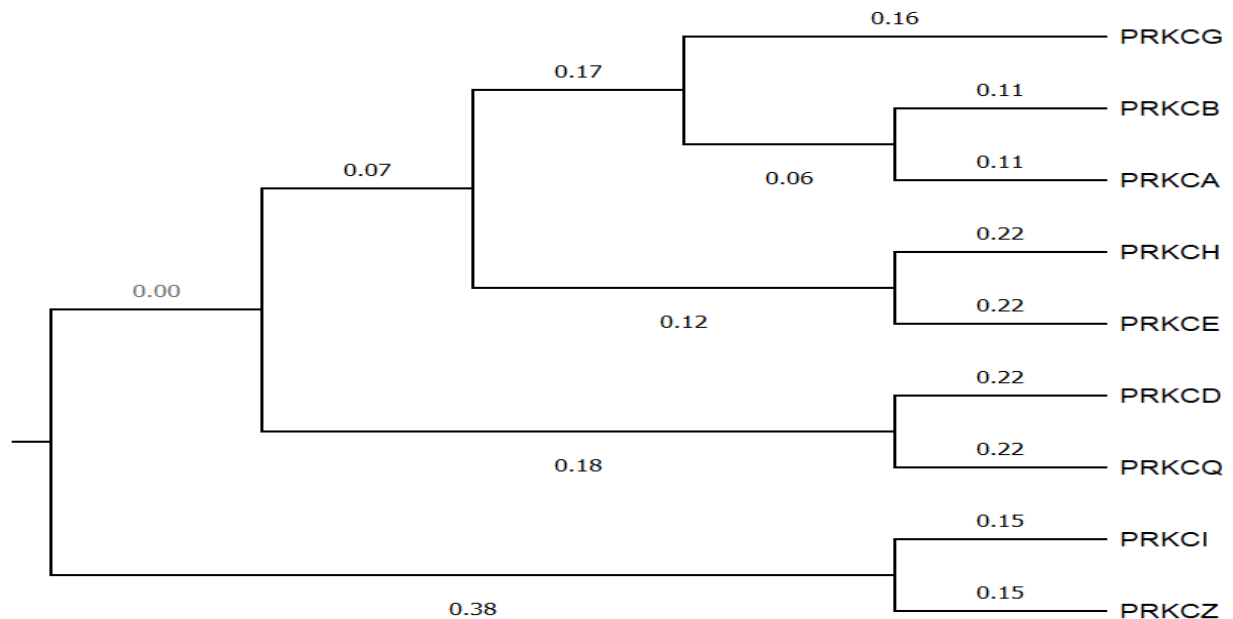


Figure 10 Represents the Phylogenetic Tree of the PKCs proteins. All the PKCs are originated from common root and then evolve into three different classes i.e., cPKCs, nPKCs and aPKCs.

4.3 Damaging SNPs

The Ensemble genome browser provides a total of 429 non-synonymous SNPs which were subjected to six different tools to analyze their impact on protein structure and function. Among the 405 nsSNPs 16 SNPs were detected to be pathogenic/deleterious after analyzing on six different tools i.e., PredictSNP2, CADD, DANN, FATHMM, FunSeq2 and GWAVA. Table 3 represent the detail information of the all the 16 SNPs that were predicted to be disease causing. Besides non-synonymous SNPs Ensemble genome browser also provides SNPs in intronic region, 3' and 5' prime UTRs and synonymous SNPs etc and their data are show in fig 11.

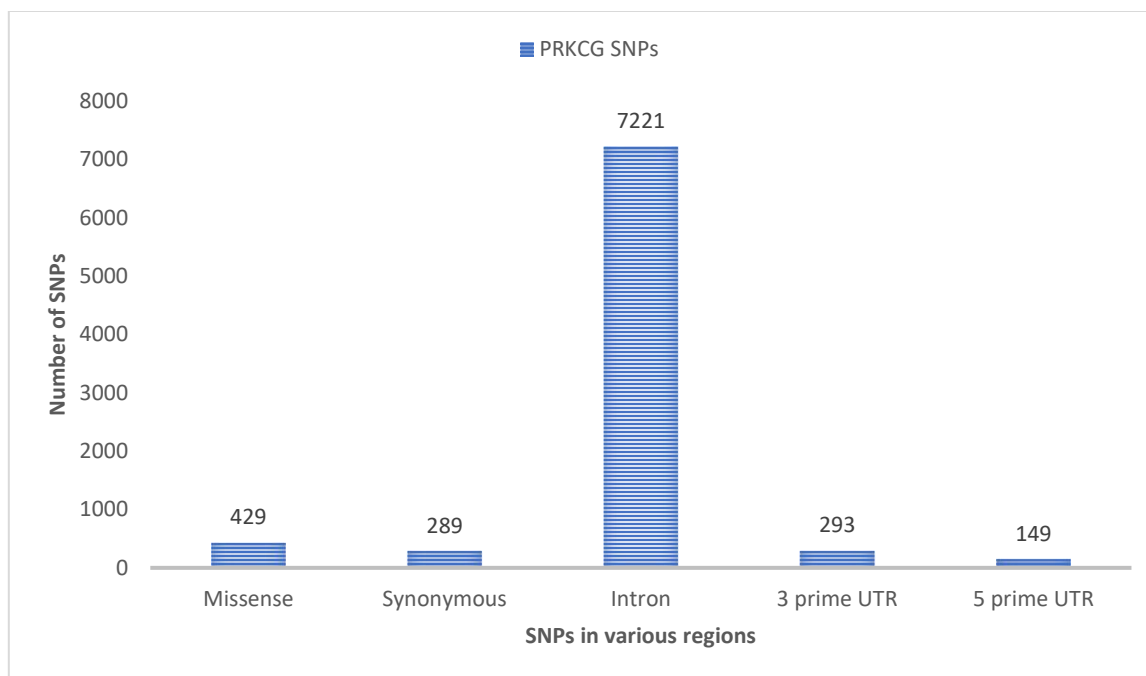


Figure 11 Graphical representation of PRKCG SNPs

Table 3 Pathogenic nsSNPs based on six different tools

Variant	PredictSNP2	CADD	DANN	FATHMM	FunSeq2	GWAVA
19:53882640, G→C	Deleterious	Deleterious	Deleterious	Deleterious	Deleterious	Deleterious
19: 53882648, T→A	Neutral	Deleterious	Neutral	Neutral	Deleterious	Deleterious
19: 53889693, G→A	Deleterious	Deleterious	Deleterious	Neutral	Deleterious	Deleterious
19: 53889719, G→A	Deleterious	Deleterious	Deleterious	Deleterious	Deleterious	Deleterious
19: 53889734, G→C	Deleterious	Deleterious	Neutral	Deleterious	Deleterious	Nil
19: 53889743, T→A	Deleterious	Deleterious	Deleterious	Deleterious	Deleterious	Nil
19: 53889743, T→C	Deleterious	Deleterious	Deleterious	Deleterious	Deleterious	Nil
19: 53889901, T→A	Neutral	Deleterious	Neutral	Neutral	Deleterious	Deleterious
19: 53889936, T→C	Deleterious	Deleterious	Deleterious	Deleterious	Deleterious	Nil

19: 53889963, G→A	Deleterious	Deleterious	Deleterious	Neutral	Deleterious	Nil
19: 53889963, G→T	Deleterious	Deleterious	Deleterious	Deleterious	Deleterious	Nil
19: 53898095, A→G	Deleterious	Deleterious	Deleterious	Deleterious	Deleterious	Deleterious
19: 53898097, G→A	Deleterious	Deleterious	Deleterious	Deleterious	Deleterious	Deleterious
19: 53900612, G→T	Deleterious	Deleterious	Neutral	Deleterious	Deleterious	Deleterious
19: 53906342, G→A	Deleterious	Deleterious	Deleterious	Deleterious	Deleterious	Deleterious
19: 53906729, T→C	Neutral	Deleterious	Deleterious	Neutral	Deleterious	Nil

The above SNPs were further filtered out and only those SNPs were selected which were predicted to be damaging by all the six tools that were used and their data are given in table 4.

Table 4 Filtered nsSNPs after applying filters

Variants	PredictSNP2	CADD	DANN	FATHMM	FunSeq2	GWAVA
19:53882640, G→C	Deleterious	Deleterious	Deleterious	Deleterious	Deleterious	Deleterious
19:53889719, G→A	Deleterious	Deleterious	Deleterious	Deleterious	Deleterious	Deleterious
19:53898095, A→G	Deleterious	Deleterious	Deleterious	Deleterious	Deleterious	Deleterious
19: 53898097, G→A	Deleterious	Deleterious	Deleterious	Deleterious	Deleterious	Deleterious
19:53906342, G→A	Deleterious	Deleterious	Deleterious	Deleterious	Deleterious	Deleterious

4.4 Effect Of nsSNPs on PRKCG Structure and Function

The effect of missense SNPs on protein stability, structure and functions were analyze by three different tools i.e. I Mutant, MutPred and HOPE. I Mutant results shows that to which degree the nsSNPs can change the stability of protein and hence the protein function is closely linked with its structure so it may alter its function too. MutPred and HOPE demonstrated that amino acid change at position 359 (*rs1331234028*) can results in loss of

protein kinase domain interaction with ATP. Table 5, 6 and figure 12 shows changes in the stability, energy, and alteration of other protein functions upon mutation.

Table 5 I-Mutant Effect of nsSNPs on protein stability.

SNP IDs	Residual Changes	Stability	RI	DDG Values (Kcal/mol)
rs758426250	C49S	Decrease	3	-0.61
rs386134164	G123R	Increase	1	-0.25
rs1331234028	K359R	Decrease	0	-2.30
rs386134171	G360S	Decrease	0	-1.06
rs1568764306	R597H	Decrease	7	-0.94

Table 6 Shows the list of possible alteration in the protein when lysine is changed with arginine at 359 position and their P-values estimated by MutPred2

Residual change	Mechanisms	P-Values
K359R	Loss of ubiquitination at K359	P = 0.027
	Gain of methylation at K359	P = 0.0351
	Gain of sheets	P = 0.0827
	Gain of phosphorylation at S361	0.0876
	Gain of MoRF binding	0.1603

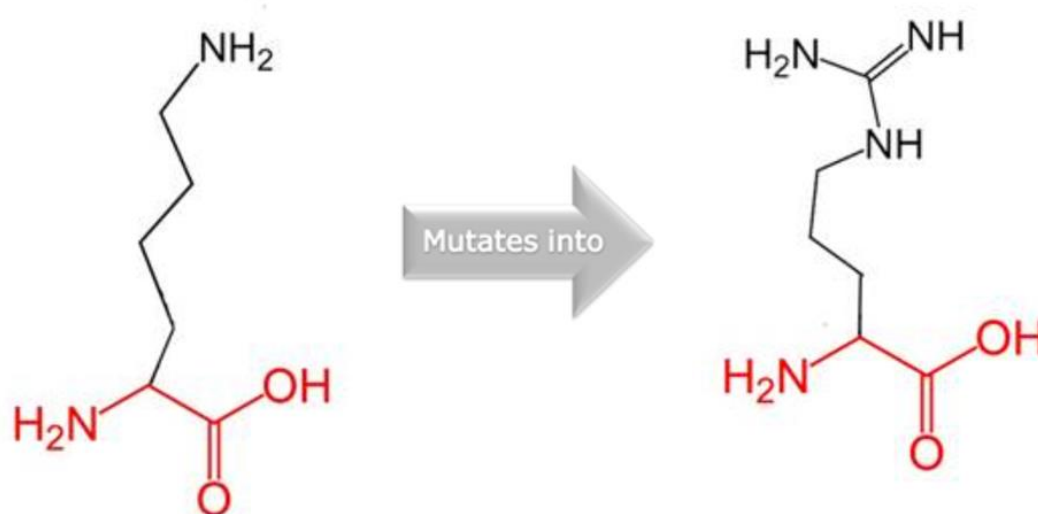


Figure 12 shows Lysine on the right side which in mutated to arginine located on the left side. The size of arginine is larger from lysine as two extra NH groups attachment.

4.5 MD Simulation Results

After the simulation was run for both wild and mutated protein, several files of important data were generated. The data in those files were plot on graphs to interpret simulation results. Four parameters were considered i.e., Root mean square deviation (RMSD), Root mean square fluctuation (RMSF), Radius of gyration and No. of hydrogen bonds to analyze the difference in wild type and mutated protein.

4.5.1 RMSD Analysis

Root mean square deviation (RMSD) shows the deviation of different atoms in protein from its mean position. RMSD analysis of the wild and mutated protein revealed that mutated protein deviate significantly from its reference position compared to wild type. Within 0.3 nanosecond the deviation is observed in the mutated protein and the pattern is followed till the end with highest deviation 1.39nm at 19 nanosecond as shown in figure 13.

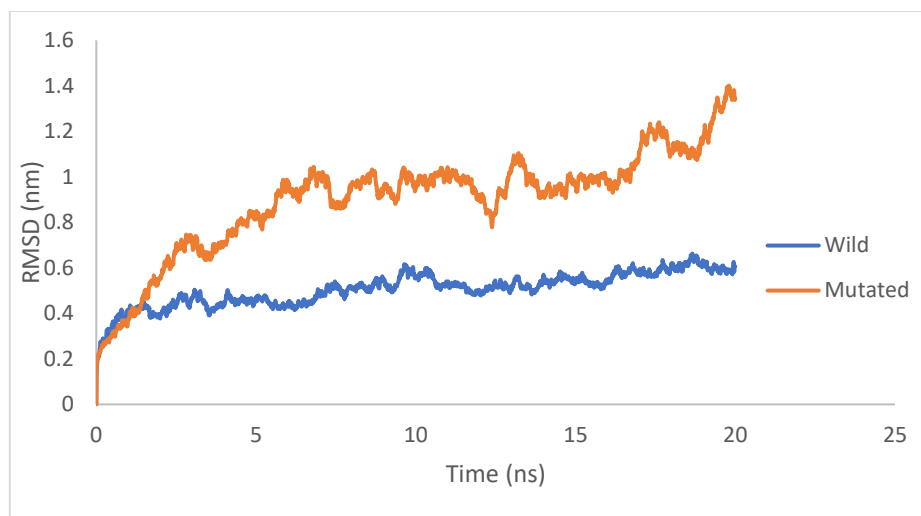


Figure 13 RMSD graph representing the significance difference in the deviation pattern between wild and mutated protein over the time.

4.5.2 RMSF Analysis

Root mean square fluctuation (RMSF) shows the fluctuation of individual residues from its mean position. RMSF analysis shows the difference in the fluctuation of wild and mutated protein residues. The region from 170-267 and 448-656 residues of the mutated protein has significance fluctuation from its mean point, which indicates that the protein structure expands over the time. The comparison between wild and mutated protein residues' fluctuation is shown in figure 14.

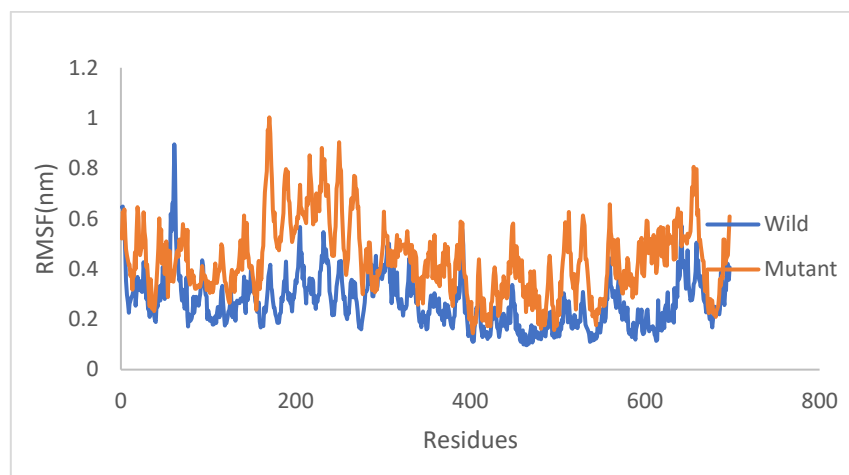


Figure 14 Amino acid residues of both wild and mutated protein was plot on x-axis against RMSF values on y-axis to analyze the difference in the fluctuation of both proteins from the reference point.

4.5.3 Radius of Gyration

Radius of gyration (R_g) represent the radial distance of an all the atoms present in the protein from their common axis. The evaluation of radius of gyration calculated for both wild and mutated protein shows a sharp increase in mutated protein peak up to 3.49 nm at 2.3 ns and the gradually decrease to 3.3 nm as simulation run for 3.9 ns. From 6.8 to 12.9 nm the gyration of mutated protein is seemed to be at a steady phase from there gradual decrease to 3.1 nm occurs as the simulation reached to 13.3 ns and then radius of gyration become stable till 19.2 ns, but at the end a significant decrease is shown. This shows that mutated protein loss its compactness at the start of simulation and became more compacted at the end as shown in figure 15. The difference in the wild and mutated protein R_g shown here is the steady phase of gyration in wild protein that is missing in mutated case.

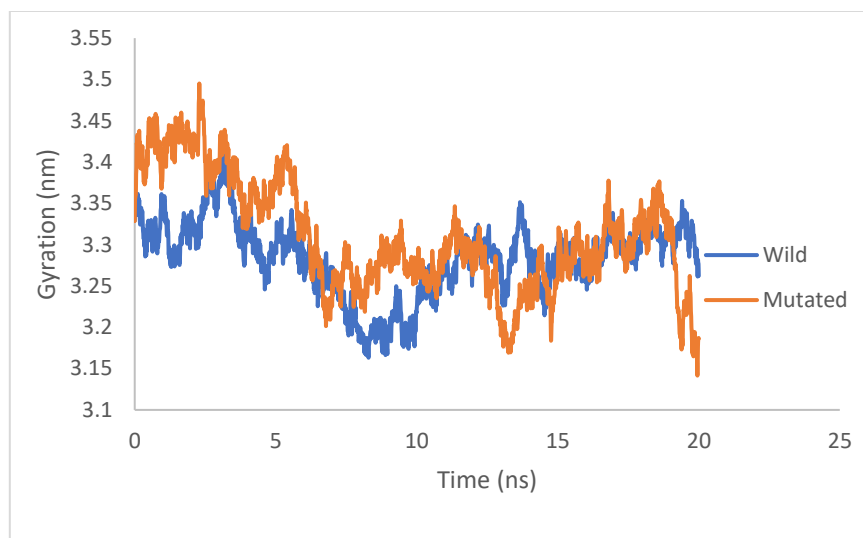


Figure 15 Radius of gyration of both wild and mutated protein shows the compactness of protein in a dynamic setting as the simulation proceeds.

4.5.4 Number of Hydrogen Bonds

The hydrogen bonds number in mutated and wild PKC gamma shows no significance difference as only a single amino acid was changed. The lines of both wild type and mutated proteins are overlapped over each other as shown in figure 16 shows that there is no mark difference.

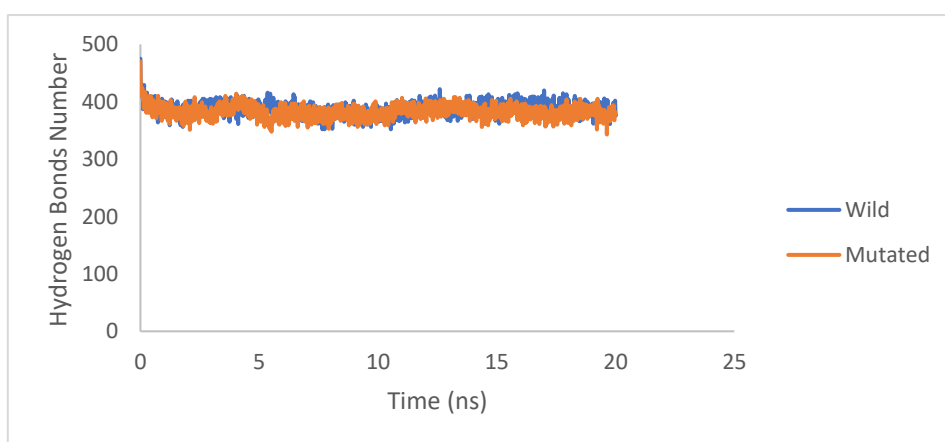


Figure 16 Represents the difference in the number of hydrogen bonds between wild and mutated protein.

4.6 AdmetSAR Analysis of a Drug

AdmetSAR analysis of the ligand shows the physio-chemical properties of the ligand. The AdmetSAR report also provides regression properties, and ADMET (Absorption, Distribution, Metabolism, Excretion & Toxicity) properties of the drug,

4.6.1 Lipinski's Rule of Five

The Lipinski's Rule of five shows the physio-chemical properties the drug and i.e., molecular weight, lipophilicity, hydrogen bond acceptor, hydrogen bond donor and rotatable bonds present in the drug. The drug is considered an optimum if its molecular weight is less than 500 Dalton, hydrogen bonds acceptor is less than 10, less than 5 hydrogen bond acceptor and AlogP less than 5 (C. A. Lipinski, Lombardo, Dominy, & Feeney, 2001). The properties predicted by AdmetSAR for our drug and their values are given in table 7.

Table 7 Represent the physio-chemical properties of the drug and their values predicted by AdmetSAR.

Lipinski's Rule of Five		
S.NO	Characteristics	Values
1	Molecular Weight	692.21
2	AlogP	3.53
3	H-Bond Acceptor	10
4	H-Bond Donor	2
5	Rotatable Bonds	5

4.6.2 Regression Analysis

Regression analysis shows that how the drug interacts with biomolecules of the body. AdmetSAR report shows the predicted properties i.e., solubility, binding to plasma membrane oral toxicity, etc. of the drug along with their values and units. Table 8 shows the detail of regression properties.

Table 8 Shows the regression properties predicted by AdmetSAR.

Regression Properties			
S.NO	Properties	Values	Unit
1	Water Solubility	-3.723	logS
2	Plasma Protein Binding	1.313	100%
3	Acute Oral Toxicity	3.893	mol/kg
4	Tetrahymena pyriformis	0.392	pIGC50 (ug/L)

5.6.3 ADMET Properties

AdmetSAR provides the pharmacokinetic properties i.e., absorption, distribution, metabolism, excretion, and toxicity of our drug and predicted that it may cross blood brain barrier, no carcinogenicity, and category III oral toxicity etc. The detail of these properties is given in table 9.

Table 9 Shows the pharmacokinetic properties of the drug.

S.NO	Properties	Values	Probability
-------------	-------------------	---------------	--------------------

1	Blood Brain Barrier	+	0.9600
2	Human Oral Bioavailability	-	0.6571
3	Subcellular localization	Lysosomes	0.5455
4	Carcinogenicity	-	0.8857
5	Acute Oral Toxicity (c)	III	0.5724
6	Hepatotoxicity	+	0.9000

4.7 Interpretation of Protein-ligand Interaction

The predicted protein-ligand interactions are given in table 10 and one which was selected is highlighted in red and figure 17 shows the protein-ligand binding predicted by CB-dock at lowest possible energy.

LigPlot+ represented ligand-protein hydrophobic interaction (semi-spiked circle) and hydrogen bonding (doted green lines), the distance between amino acids and the interacting atoms of the ligand in angstrom. Nine amino acids shown in semi-spiked circle are involved in hydrophobic interaction with the carbon atoms present in the ligand. Fig 18A and 18B represent the 2d and 3d depiction of receptor and ligand binding.

Table 10 CB Dock table representing possible interaction score and cavity size.

S.NO	Vina Score	Cavity Size
1	-9.2	2411
2	-8.8	1266
3	-8.4	1277
4	-8	13287
5	-6.9	3082

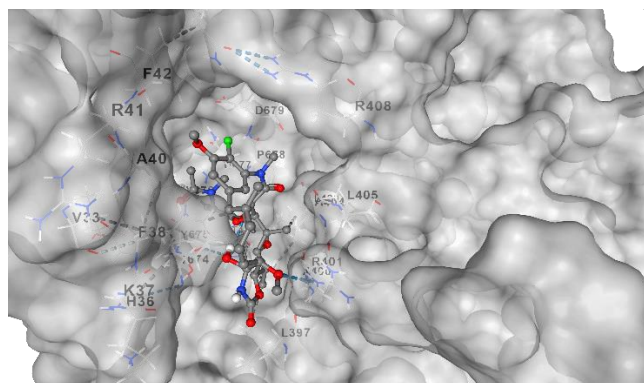


Figure 17 Shows the drug binding pocket of the receptor in surface form and the attached ligand in sticks and balls format.

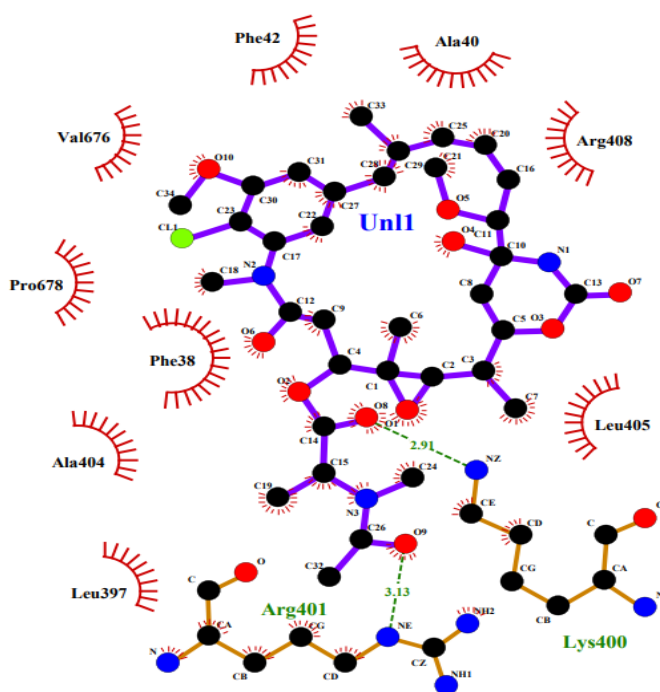


Fig 18A. Protein-ligand bonding and molecular interaction. Amnio acid with hydrophobic interaction, Hydrogen bonding, covalent bonding ligand and non-ligand, distance of hydrogen bonding are shown in semi-spiked circle, green dotted lines, orange, and purple lines, angstrom (3.13 & 2-91) and carbon, nitrogen and oxygen molecules are represented in black, blue, and red circles.

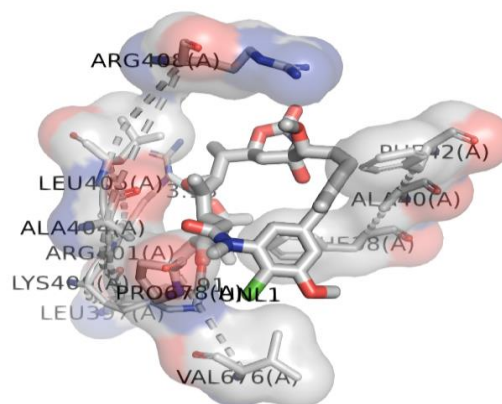


Figure 18B 3d representation of protein-ligand bonding via PyMOL.

4.8 Genotype Data of HCC And Control Samples

After analysis of the HCC genotype data the results showed SNP in homozygous wild form (AA) could be highly associated with the disease as compared to homozygous GG and heterozygous AG based on odd value and relative risk 5.194 and 2.287 respectively, with P-value <0.0001. The polymorphism in this allele may reduce the risk of disease occurrence.

Table 11 shows the genotype data of patients and control.

Table 11 Genotype Data of Patient and Control

Genotype	Frequency Distribution		Odd Ratio		Relative Risk		P-Value
	Patients	Control	Value	CI 95%	Value	CI 95%	
AG	19%	33%	0.3827	0.2033 to 0.7236	0.5885	0.3882 to 0.8471	0.0046
GG	11%	31%	0.2751	0.1246 to 0.5777	0.4650	0.2675 to 0.7475	0.0008

AA	70.00%	31%	5.194	2.887 9.407	to	2.287	1.674 3.203	to	<0.0001
----	--------	-----	-------	----------------	----	-------	----------------	----	---------

4.8.1 Data Based on Gender

The comparison of male/female patient with control replicate the above results mentioned in table 12. Homozygous allele AA in both male and female were found to be associated with the disease. The OR and RR for was was 6.021 and 2.310 respectively, and that of female was 4.737 (OR) and 2.291 (RR). The P-value for male and female having allele AA was <0.0001 and 0.0002 respectively which shows the significance of the results. The Allelic data for gender is represented in table 12.

Table 12 Allelic Data Based on Gender

Patient-Control Analysis Based on Gender							
Genotype	Frequency Distribution		Odd Ratio		Relative Risk		P-Value
	Patients	Control	Value	CI 95%	Value	CI 95%	
AG (M)	24.00%	43.48%	0.4105	0.1768 to 0.9697	0.631 6	0.3734 to 0.9871	0.0528
GG (M)	8.00%	30.43%	0.1988	0.06748 to 0.6852	0.376 8	0.1503 to 0.7927	0.0078
AA (M)	68.00%	26.09%	6.021	2.551 to 14.71	2.310	1.527 to 3.657	<0.0001
AG (F)	14.00%	33.33%	0.3256	0.1298 to 0.8953	0.514 4	0.2558 to 0.9183	0.0237

GG (F)	14.00%	31.48%	0.3543	0.1408 to 0.9082	0.542 6	0.2704 to 0.9627	0.0390
AA (F)	72.00%	35.19%	4.737	2.030 to 10.36	2.291	1.456 to 3.785	0.0002

4.8.2 Age Group Data

The analysis of genotype data based on age group also replicate the same results as in gender.

The odd values, relative risk and P-values of different age group showed that allele AA has strong association with the disease occurrence. The detail information of allelic data is given in table 13.

Table 13 Allelic Data of Different Age Groups

Patient-Control Analysis Based on Age Group							
Genotype	Frequency Distribution		Odd Ratio		Relative Risk		P-Value
	Patients	Control	Value	CI 95%	Value	CI 95%	
AG 1-19	0.00%	100.00%	0.000	0.000 to 9.000	0.000	0.000 to 1.921	>0.9999
GG 1-19	Nil	Nil	Nil	Nil	0.000	0.000 to 1.000	>0.9999
AA 1-19	100.00%	0.00%	Infinity	0.1111 to Infinity	Infinity	0.5206 to Infinity	>0.9999
AG 20-39	18.75%	36.36%	0.4038	0.1644 to 0.9920	0.6185	0.3377 to 1.014	0.0654
GG 20-39	10.42%	34.09%	0.2248	0.08391 to 0.6931	0.4186	0.1838 to 0.8160	0.0103
AA 20-39	70.83%	29.55%	5.791	2.396 to 14.43	2.325	1.501 to 3.805	0.0001
AG 40-59	20.41%	33.33%	0.5128	0.1945 to 1.334	0.1743	0.3948 to 1.122	0.1743

GG 40-59	12.24%	31.25%	0.3070	0.1065 to 0.8629	0.5050	0.2388 to 0.9249	0.0279
AA 40-59	67.35%	35.42%	3.761	1.571 to 8.402	1.939	1.272 to 3.087	0.0023
AG 60+	0.00%	71.43%	0.000	0.000 to 1.530	0.000	0.000 to 1.180	0.1667
GG 60+	0.00%	14.29%	0.000	0.000 to 31.50	0.000	0.000 to 6.405	>0.9999
AA 60+	100.00%	14.29%	Infinity	1.150 to Infinity	Infinity	1.321 to Infinity	0.0833

4.9 Analysis of ALT In Patient vs Control

The of ALT level of patients were diagnosed to be significantly higher when compared with the control sample. The average concentration of ALT in patients were 106.84 U/L which were significantly higher from the normal ALT range which is 7-40 U/L. The control sample shows that ALT level was under 40. Figure 19 represent the comparison of ALT concentration in patient vs control.

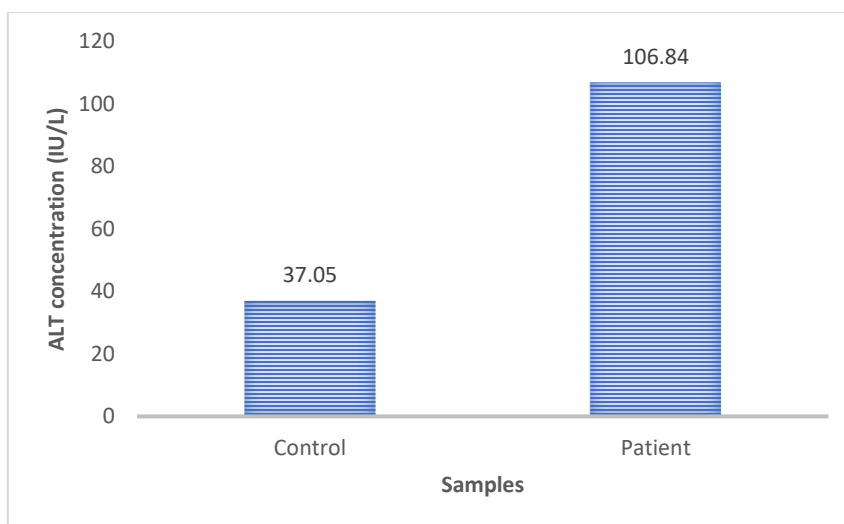


Figure 19 Comparison of ALT concentration in patients and control

4.10 Viral Load Analysis of Patients with Different Alleles

Viral Load of in patients was provided by qRT-PCR. The analysis of viral load against genotype Shows significant difference. Average of viral load for genotype AA, GG and AG was taken and then analyzed which shows that patients with AG allele has significantly high (819438471 cpoies/ml) viral load compared to patients with AA and GG alleles given in figure 20 which suggests that there may be a correlation of viral load and genotype.

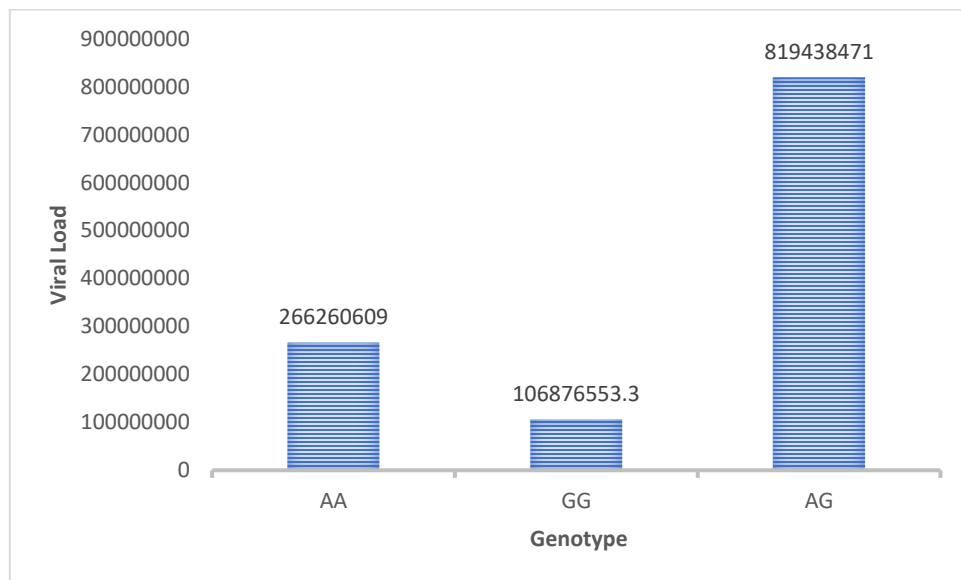


Figure 20 Correlation of viral load and Genotype

Chapter 5 Discussion

The aim of this study was to investigate the association of PKC gamma missense SNP with HCV induced Hepatocellular carcinoma. As the major problem with most the cancers is the detection of the disease in early stages and HCC is no more different. The genotype association of PKC gamma HCC can be used as prognostic marker for the early diagnosis of the disease. PRKCG protein model predicted via I-TASSER belong to conventional PKC (cPKC) class consist of PKC alpha, PKC beta1 & 2 and PKC Gamma. The mutation in PRKCG at position 359 from lysin to arginine falls within the kinase domain which is present in all the members of conventional PKC (A. C. J. C. r. Newton, 2001). The model we chose was based on the C-score (-2.53) and InterPro prediction. It has been previously established that there is 40% similarity in protein sequence between cPKC and protein kinase A. I-TASSER has also been previously used in different studies to predict protein 3d model i.e., TAGAP, CCR6 and TOX3 etc. (Akhtar, Jamal, Jamal, et al., 2019; Akhtar, Jamal, ud Din, et al., 2019; Arshad, Bhatti, & John, 2018). The selection of I-TASSER was based on Automated assessment of protein 3D structure prediction in CASP which considered various parameters to confer accuracy of the predictor.

As the target of the study was to correlate the single nucleotide polymorphism with HCC so this purpose SNPs in PRKCG was retrieved from Ensemble Genome Browser. Only missense SNPs were selected as they have direct impact on protein structure and may alter its function to some extent. The retrieved non-synonymous SNPs were subjected to different tools i.e., PredictSNP2, CADD, DANN, FATHMM, FunSeq2 and GWAVA to predict the impact of single nucleotide polymorphism on protein. 16 SNPs that were selected from large pool of 429 missense SNPs were predicted to have deleterious effect by at least 3 tools. The

list was then further narrowed down to just 5 SNPs and then one SNP (rs1331234028) was selected for further analysis. The correlation of missense mutation at position 463 from aspartic acid to histidine PKC alpha a member of conventional PKC with chordoid glioma was established as it has been studied that the mutated PRKCA can significantly increase the level of phosphorylated ERK and can induce cancer (Goode et al., 2018).

The structural and functional analysis of rs1331234028 (K359R) was performed via I-Mutant, HOPE and MutPred which predict that mutation at this position may decrease the stability of the protein and the DDG value and reliability index (RI) for K359R calculated by I-Mutant was -2,30 Kcal/mol and 0. As the two residues differ in size so it was estimated by HOPE that it might disturb the function of kinase domain of the protein considering the mutation in that region. MutPred predicted that substitution of lysine with arginine at position 359 in PRKCG may disturb the function of the protein and may cause Loss of ubiquitination at K359 (P = 0.027); Gain of methylation at K359 (P = 0.0351); Gain of sheet (P = 0.0827); Gain of phosphorylation at S361 (P = 0.0876); Gain of MoRF binding (P = 0.1603). All these predictions made by HOPE, I-Mutant and MutPred implicate that the impact of single amino acid change is not restricted to that residue but can also affect the function of other residues.

The brief investigation of Molecular Dynamic simulations estimated that the mutation of PKC gamma at position 359 from lysine (K) to Arginine (R) may alter the structure of the protein. A significance difference was found in the analysis of RMSD, RMSF and Radius of gyration between wild and mutated protein. MD simulation also revealed that the impact of single amino acid change may not be restricted to that specific position as seen in simulation results.

As the in-silico analysis estimated that mutation in PRKCG (K359R) may alter the structure and hence the function of the protein, to validate these predictions two sets of primers (two outer and two inner) were designed via Primer1 against rs1331234028 to find the correlation between allele change hepatocellular carcinoma. DNA extraction followed by tetra ARMS-PCR was performed for this purpose. The analysis of PCR results revealed that the wild type allele AA has strong correlation, OD (5.194), relative risk (2.287) and P-value >0.0001 , with HCC compared to homozygous GG and Heterozygous AG. The results were also analyzed based on gender and age group shows difference in OD and relative risk in male and female and suggest that a male with allele AA may have at higher risk compared to female, but no clear results were achieved from analysis based on age group because of the sample size. The association of polymorphism with genetic disease give us an idea about susceptibility and can also be used for early diagnosis as the study of the osteoarthritis in Pakistani population revealed that polymorphisms in IL-6, TGF-beta-1 and CALM₁ genes were associated with the disease (Badshah et al., 2021).

It has been established that high alanine aminotransferase (ALT) level is linked with hepatitis C virus (HCV) hepatocellular carcinoma (HCC) and can lead to the disease rapidly (Tarao et al., 1999). So, the ALT test was performed for both patients and control and the results shown significant difference in the level of ALT. The average level of ATL for patients was 106.84 IU/L compared to control 37.05 IU/L.

The association of viral load with genotype was performed to analyze the link of genotype with viral load. Our results demonstrated that patients with genotype AG have high viral load followed by AA and then GG. Literature shows clearance of HCV viral RNA in patients

coinfecting with HCV/HIC having rs12979860 polymorphism CC genotype (Lapiński, Pogorzelska, Kowalczyk, Nikliński, & Flisiak, 2013).

After invitro analysis of the SNP and its association with the disease, docking was performed via CB-Dock. Maytansine was used as ligand for PRKCG and was selected based on AdmetSAR analysis which estimates the biocompatibility and drugability of the potential therapeutic drug. According to Lipinski's rule of five a drug can be used for therapeutic purpose if the molecular weight is less than 500, $\text{LogP} < 5$, hydrogen bond donor < 5 and hydrogen bond acceptor < 10 (Christopher A Lipinski, Lombardo, Dominy, & Feeney, 1997). AdmetSAR results predicted that Maytansine can be used as drug as it fulfills the above criteria, and the literature also shows that conjugation of Maytansine with humanized C242 antibody has potential anticancer activity and biocompatible (Gerber, Koehn, & Abraham, 2013). Maytansine was docked with PRKCG and the protein ligand binding at lower energy was selected as it is a known phenomenon that interaction with lower energy is stable. PKC gamma spectroscopic analysis is required to fully reveal the structure of the protein. The analysis of change in the proteomic profile of the PKC gamma upon missense mutation may further help in understanding the molecular mechanism of the protein and its association with HCC.

5.1 Conclusion

Missense mutation in PKC gamma protein rs1331234028 variant AA was found to be pathogenic and strongly associated with hepatocellular carcinoma. The structure of the protein was predicted, and structural and functional analysis shows that the protein overall stability was decreased upon mutation. The SNP identified may be used as genetic marker

which can help us in the early diagnosis of the hepatocellular carcinoma and potential drug target. Maytansine-protein docking was performed to proposed that this protein can used as potential therapeutic drug and promising in-silico results were achieved. The expression profile of the PKC gamma upon this mutation needs to be explore which may open new ways in the cancer therapeutic field.

References

- Adachi, N., Kobayashi, T., Takahashi, H., Kawasaki, T., Shirai, Y., Ueyama, T., . . . Saito, N. (2008). Enzymological analysis of mutant protein kinase Cy causing spinocerebellar ataxia type 14 and dysfunction in Ca²⁺ homeostasis. *Journal of Biological Chemistry*, *283*(28), 19854-19863.
- Akamine, P., Madhusudan, Wu, J., Xuong, N. H., Ten Eyck, L. F., & Taylor, S. S. (2003). Dynamic features of cAMP-dependent protein kinase revealed by apoenzyme crystal structure. *J Mol Biol*, *327*(1), 159-171. doi:10.1016/s0022-2836(02)01446-8
- Akhtar, M., Jamal, T., Jamal, H., Din, J. U., Jamal, M., Arif, M., . . . Jalil, F. J. I. j. o. i. (2019). Identification of most damaging nsSNPs in human CCR6 gene: In silico analyses. *46*(6), 459-471.
- Akhtar, M., Jamal, T., ud Din, J., Hayat, C., Rauf, M., ul Haq, S. M., . . . Jalil, F. J. J. o. g. (2019). An in silico approach to characterize nonsynonymous SNPs and regulatory SNPs in human TOX3 gene. *98*(5), 1-10.
- Aljagthmi, A. A., Hill, N. T., Cooke, M., Kazanietz, M. G., Abba, M. C., Long, W., & Kadakia, M. P. (2019). ΔNp63α suppresses cells invasion by downregulating PKCγ/Rac1 signaling through miR-320a. *Cell death & disease*, *10*(9), 1-14.
- Alkon, D. L. (1989). Memory storage and neural systems. *Scientific American*, *261*(1), 42-51.
- Arshad, M., Bhatti, A., & John, P. J. P. o. (2018). Identification and in silico analysis of functional SNPs of human TAGAP protein: A comprehensive study. *13*(1), e0188143.
- Asai, H., Hirano, M., Shimada, K., Kiriya, T., Furiya, Y., Ikeda, M., . . . Konishi, N. (2009). Protein kinase Cy, a protein causative for dominant ataxia, negatively regulates nuclear import of recessive-ataxia-related aprataxin. *Human molecular genetics*, *18*(19), 3533-3543.
- Ashendel, C. L. (1985). The phorbol ester receptor: a phospholipid-regulated protein kinase. *Biochimica et Biophysica Acta (BBA)-Reviews on Biomembranes*, *822*(2), 219-242.
- Badshah, Y., Shabbir, M., Hayat, H., Fatima, Z., Burki, A., Khan, S., . . . Research. (2021). Genetic markers of osteoarthritis: early diagnosis in susceptible Pakistani population. *16*(1), 1-8.
- Balagopal, A., Thomas, D. L., & Thio, C. L. (2010). IL28B and the control of hepatitis C virus infection. *Gastroenterology*, *139*(6), 1865-1876.
- Barnett, M. E., Madgwick, D. K., & Takemoto, D. J. (2007). Protein kinase C as a stress sensor. *Cellular signalling*, *19*(9), 1820-1829.
- Barroso, I., Gurnell, M., Crowley, V. E. F., Agostini, M., Schwabe, J. W., Soos, M. A., . . . O'Rahilly, S. (1999). Dominant negative mutations in human PPARγ associated with severe insulin resistance, diabetes mellitus and hypertension. *Nature*, *402*(6764), 880-883. doi:10.1038/47254

- Bekker, H., Berendsen, H., Dijkstra, E., Achterop, S., Vondrumen, R., VANDERSPOEL, D., . . . Renardus, M. (1993). *Gromacs-a parallel computer for molecular-dynamics simulations*. Paper presented at the 4th International Conference on Computational Physics (PC 92).
- Bell, R. M., & Burns, D. J. (1991). Lipid activation of protein kinase C. *Journal of Biological Chemistry*, *266*(8), 4661-4664.
- Bendl, J., Musil, M., Štourač, J., Zendulka, J., Damborský, J., & Brezovský, J. J. P. c. b. (2016). PredictSNP2: a unified platform for accurately evaluating SNP effects by exploiting the different characteristics of variants in distinct genomic regions. *12*(5), e1004962.
- Black, A. R., & Black, J. D. (2012). Protein kinase C signaling and cell cycle regulation. *Front Immunol*, *3*, 423. doi:10.3389/fimmu.2012.00423
- Black, A. R., & Black, J. D. J. F. i. i. (2013). Protein kinase C signaling and cell cycle regulation. *3*, 423.
- Blum, M., Chang, H.-Y., Chuguransky, S., Grego, T., Kandasamy, S., Mitchell, A., . . . Raj, S. (2021). The InterPro protein families and domains database: 20 years on. *Nucleic Acids Research*, *49*(D1), D344-D354.
- Brumfeld, V., & Lester, D. S. (1990). Protein kinase C penetration into lipid bilayers. *Archives of biochemistry and biophysics*, *277*(2), 318-323.
- Capriotti, E., & Altman, R. B. (2011). Improving the prediction of disease-related variants using protein three-dimensional structure. *BMC bioinformatics*, *12*(S4), S3.
- Capriotti, E., Fariselli, P., & Casadio, R. J. N. a. r. (2005). I-Mutant2.0: predicting stability changes upon mutation from the protein sequence or structure. *33*(suppl_2), W306-W310.
- Chasman, D., & Adams, R. M. (2001). Predicting the functional consequences of non-synonymous single nucleotide polymorphisms: structure-based assessment of amino acid variation. *Journal of molecular biology*, *307*(2), 683-706.
- Chedid, M. F., Krueel, C. R., Pinto, M. A., Grezzana-Filho, T. J., Leipnitz, I., Krueel, C. D., . . . Chedid, A. D. J. A. A. B. d. C. D. (2017). Hepatocellular carcinoma: diagnosis and operative management. *30*, 272-278.
- Cheng, F., Li, W., Zhou, Y., Shen, J., Wu, Z., Liu, G., . . . Tang, Y. (2012). admetSAR: a comprehensive source and free tool for assessment of chemical ADMET properties. *J Chem Inf Model*, *52*(11), 3099-3105. doi:10.1021/ci300367a
- Chia, T. S., Wong, K. F., & Luk, J. M. J. H. R. (2019). Molecular diagnosis of hepatocellular carcinoma: trends in biomarkers combination to enhance early cancer detection. *5*.
- Collins, A., & Ke, X. J. T. O. B. J. (2012). Primer1: primer design web service for tetra-primer ARMS-PCR. *6*(1).
- Collins, F. S., Guyer, M. S., & Chakravarti, A. (1997). Variations on a theme: cataloging human DNA sequence variation. *Science*, *278*(5343), 1580-1581.
- Coussens, L., Parker, P. J., Rhee, L., Yang-Feng, T. L., Chen, E., Waterfield, M. D., . . . Ullrich, A. (1986). Multiple, distinct forms of bovine and human protein kinase C suggest diversity in cellular signaling pathways. *Science*, *233*(4766), 859-866. doi:10.1126/science.3755548
- Coussens, L., Parker, P. J., Rhee, L., Yang-Feng, T. L., Chen, E., Waterfield, M. D., . . . Ullrich, A. (1986). Multiple, distinct forms of bovine and human protein kinase C suggest diversity in cellular signaling pathways. *Science*, *233*(4766), 859-866.
- Cutler Jr, R. E., Maizels, E. T., Brooks, E. J., Mizuno, K., Ohno, S., & Hunzicker-Dunn, M. (1993). Regulation of δ protein kinase C during rat ovarian differentiation. *Biochimica et Biophysica Acta (BBA)-Molecular Cell Research*, *1179*(3), 260-270.

- Devilee, P., & Rookus, M. A. (2010). A tiny step closer to personalized risk prediction for breast cancer. In: Mass Medical Soc.
- Dowling, C. M., Hayes, S. L., Phelan, J. J., Cathcart, M. C., Finn, S. P., Mehigan, B., . . . Kiely, P. A. (2017). Expression of protein kinase C gamma promotes cell migration in colon cancer. *Oncotarget*, *8*(42), 72096.
- Evan, G., & Littlewood, T. (1998). A matter of life and cell death. *Science*, *281*(5381), 1317-1322.
- Evan, G. I., & Vousden, K. H. (2001). Proliferation, cell cycle and apoptosis in cancer. *Nature*, *411*(6835), 342-348.
- Fabbro, D., Ruetz, S., Bodis, S., Pruschy, M., Csermak, K., Man, A., . . . Meyer, T. (2000). PKC412--a protein kinase inhibitor with a broad therapeutic potential. *Anticancer Drug Des*, *15*(1), 17-28.
- Finniss, S., Lee, H. K., Xiang, C., Cazacu, S., Zenklusen, J. C., Fine, H. A., . . . Brodie, C. (2006). PKC gamma has tumor suppressor activity in gliomas. In: AACR.
- FLEMING, I., MacKENZIE, S. J., VERNON, R. G., ANDERSON, N. G., HOUSLAY, M. D., & KILGOUR, E. (1998). Protein kinase C isoforms play differential roles in the regulation of adipocyte differentiation. *Biochemical Journal*, *333*(3), 719-727.
- Forner, A., Llovet, J. M., & Bruix, J. (2012). Hepatocellular carcinoma. *Lancet*, *379*(9822), 1245-1255. doi:10.1016/s0140-6736(11)61347-0
- Fu, Y., Liu, Z., Lou, S., Bedford, J., Mu, X. J., Yip, K. Y., . . . Gerstein, M. J. G. b. (2014). FunSeq2: a framework for prioritizing noncoding regulatory variants in cancer. *15*(10), 1-15.
- Gallegos, L. L., & Newton, A. C. J. I. I. (2008). Spatiotemporal dynamics of lipid signaling: protein kinase C as a paradigm. *60*(12), 782-789.
- Garczarczyk, D., Szeker, K., Galfi, P., Csordas, A., & Hofmann, J. (2010). Protein kinase C γ in colon cancer cells: Expression, Thr514 phosphorylation and sensitivity to butyrate-mediated upregulation as related to the degree of differentiation. *Chemico-biological interactions*, *185*(1), 25-32.
- Gerber, H.-P., Koehn, F. E., & Abraham, R. T. J. N. p. r. (2013). The antibody-drug conjugate: an enabling modality for natural product-based cancer therapeutics. *30*(5), 625-639.
- Goode, B., Mondal, G., Hyun, M., Ruiz, D. G., Lin, Y.-H., Van Ziffle, J., . . . Grenert, J. P. J. N. c. (2018). A recurrent kinase domain mutation in PRKCA defines chordoid glioma of the third ventricle. *9*(1), 1-8.
- Gould, C. M., Kannan, N., Taylor, S. S., & Newton, A. C. (2009). The chaperones Hsp90 and Cdc37 mediate the maturation and stabilization of protein kinase C through a conserved PXXP motif in the C-terminal tail. *J Biol Chem*, *284*(8), 4921-4935. doi:10.1074/jbc.M808436200
- Gschwendt, M., Müller, H. J., Kielbassa, K., Zang, R., Kittstein, W., Rincke, G., & Marks, F. (1994). Rottlerin, a novel protein kinase inhibitor. *Biochem Biophys Res Commun*, *199*(1), 93-98. doi:10.1006/bbrc.1994.1199
- Guertin, D. A., Stevens, D. M., Thoreen, C. C., Burds, A. A., Kalaany, N. Y., Moffat, J., . . . Sabatini, D. M. (2006). Ablation in mice of the mTORC components raptor, rictor, or mLST8 reveals that mTORC2 is required for signaling to Akt-FOXO and PKC α , but not S6K1. *Dev Cell*, *11*(6), 859-871. doi:10.1016/j.devcel.2006.10.007
- Gupta, G. P., & Massagué, J. (2006). Cancer metastasis: building a framework. *Cell*, *127*(4), 679-695.
- Han, Y., Han, Z.-Y., Zhou, X.-M., Shi, R., Zheng, Y., Shi, Y.-Q., . . . Fan, D.-M. (2002). Expression and function of classical protein kinase C isoenzymes in gastric cancer cell line and its drug-resistant sublines. *World journal of gastroenterology*, *8*(3), 441.

- He, C., Tu, H., Sun, L., Xu, Q., Gong, Y., Jing, J., . . . Yuan, Y. (2015). SNP interactions of Helicobacter pylori-related host genes PGC, PTPN11, IL1B, and TLR4 in susceptibility to gastric carcinogenesis. *Oncotarget*, *6*(22), 19017.
- Jemal, A., Bray, F., Center, M. M., Ferlay, J., Ward, E., & Forman, D. (2011). Global cancer statistics. *CA: a cancer journal for clinicians*, *61*(2), 69-90.
- Jing, J.-J., Li, M., & Yuan, Y. (2012). Toll-like receptor 4 Asp299Gly and Thr399Ile polymorphisms in cancer: a meta-analysis. *Gene*, *499*(2), 237-242.
- Johnson, K., Jones, P., Spurr, N., Nimmo, E., Davies, J., Creed, H., . . . Williamson, R. (1988). Linkage relationships of the protein kinase C gamma gene which exclude it as a candidate for myotonic dystrophy. *Cytogenetic and Genome Research*, *48*(1), 13-15.
- Kamimura, K., Hojo, H., & Abe, M. (2004). Characterization of expression of protein kinase C isozymes in human B-cell lymphoma: Relationship between its expression and prognosis. *Pathology international*, *54*(4), 224-230.
- Kashiwada, Y., Huang, L., Ballas, L. M., Jiang, J. B., Janzen, W. P., & Lee, K. H. (1994). New hexahydroxybiphenyl derivatives as inhibitors of protein kinase C. *J Med Chem*, *37*(1), 195-200. doi:10.1021/jm00027a025
- Khan, S. A., Toledano, M. B., & Taylor-Robinson, S. D. (2008). Epidemiology, risk factors, and pathogenesis of cholangiocarcinoma. *HPB (Oxford)*, *10*(2), 77-82. doi:10.1080/13651820801992641
- Kim, S., Chen, J., Cheng, T., Gindulyte, A., He, J., He, S., . . . Yu, B. J. N. a. r. (2021). PubChem in 2021: new data content and improved web interfaces. *49*(D1), D1388-D1395.
- Klein, G. (1988). Oncogenes and tumor suppressor genes. *Acta Oncologica*, *27*(4), 427-437.
- Kong, S.-S., Liu, J.-J., Yu, X.-J., Lu, Y., & Zang, W.-J. (2012). Protection against ischemia-induced oxidative stress conferred by vagal stimulation in the rat heart: involvement of the AMPK-PKC pathway. *International journal of molecular sciences*, *13*(11), 14311-14325.
- Kucukkal, T. G., Petukh, M., Li, L., & Alexov, E. (2015). Structural and physico-chemical effects of disease and non-disease nsSNPs on proteins. *Curr Opin Struct Biol*, *32*, 18-24. doi:10.1016/j.sbi.2015.01.003
- Kumar, V., Kato, N., Urabe, Y., Takahashi, A., Muroyama, R., Hosono, N., . . . Nakagawa, H. (2011). Genome-wide association study identifies a susceptibility locus for HCV-induced hepatocellular carcinoma. *Nature genetics*, *43*(5), 455-458.
- Lapetina, E., Reep, B., Ganong, B., & Bell, R. (1985). Exogenous sn-1, 2-diacylglycerols containing saturated fatty acids function as bioregulators of protein kinase C in human platelets. *Journal of Biological Chemistry*, *260*(3), 1358-1361.
- Lapiński, T. W., Pogorzelska, J., Kowalczyk, O., Nikliński, J., & Flisiak, R. (2013). SNP RS12979860 related spontaneous clearance of hepatitis c virus infection in HCV/HIV-1 coinfecting patients. *Przegl Epidemiol*, *67*(3), 407-409, 517-409.
- Lester, D. S., Doll, L., Brumfled, V., & Miller, I. R. (1990). Lipid dependence of surface conformations of protein kinase C. *Biochimica et Biophysica Acta (BBA)-Protein Structure and Molecular Enzymology*, *1039*(1), 33-41.
- Lipinski, C. A., Lombardo, F., Dominy, B. W., & Feeney, P. J. (2001). Experimental and computational approaches to estimate solubility and permeability in drug discovery and development settings. *Adv Drug Deliv Rev*, *46*(1-3), 3-26. doi:10.1016/s0169-409x(00)00129-0
- Lipinski, C. A., Lombardo, F., Dominy, B. W., & Feeney, P. J. J. A. d. d. r. (1997). Experimental and computational approaches to estimate solubility and permeability in drug discovery and development settings. *23*(1-3), 3-25.

- Liu, Y., Grimm, M., Dai, W.-t., Hou, M.-c., Xiao, Z.-X., & Cao, Y. J. A. P. S. (2020). CB-Dock: a web server for cavity detection-guided protein–ligand blind docking. *41*(1), 138-144.
- Liu, Y. R., Tang, R. X., Huang, W. T., Ren, F. H., He, R. Q., Yang, L. H., . . . Chen, G. (2015). Long noncoding RNAs in hepatocellular carcinoma: Novel insights into their mechanism. *World J Hepatol*, *7*(28), 2781-2791. doi:10.4254/wjh.v7.i28.2781
- Lu, H., Zhu, L., Lian, L., Chen, M., Shi, D., & Wang, K. (2015). Genetic variations in the PRKCG gene and osteosarcoma risk in a Chinese population: a case-control study. *Tumor Biology*, *36*(7), 5241-5247.
- Margolis, B., Rhee, S., Felder, S., Mervic, M., Lyall, R., Levitzki, A., . . . Schlessinger, J. (1989). EGF induces tyrosine phosphorylation of phospholipase C-II: a potential mechanism for EGF receptor signaling. *Cell*, *57*(7), 1101-1107.
- Mazzoni, E., Adam, A., de Kier Joffe, E. B., & Aguirre-Ghiso, J. A. (2003). Immortalized Mammary Epithelial Cells Overexpressing Protein Kinase C γ Acquire a Malignant Phenotype and Become Tumorigenic in Vivo¹ 1 University of Buenos Aires, the National Council for Scientific and Technological Research (CONICET), Ramón Carrillo-Arturo Oñativia Fellowship from Ministry of Health and the National Agency for Science and Technology Promotion (ANPCYT), from Argentina (to EBKJ) and by the Charles H. Revson Foundation (JAAG). Note: EBKJ is a member of the CONICET, Argentina. *Molecular cancer research*, *1*(10), 776-787.
- Mishima, K., Ohno, S., Shitara, N., Yamaoka, K., & Suzuki, K. (1994). Opposite effects of the overexpression of protein kinase C γ and δ on the growth properties of human glioma cell line U251 MG. *Biochemical and biophysical research communications*, *201*(1), 363-372.
- Mochly-Rosen, D. (1995). Localization of protein kinases by anchoring proteins: a theme in signal transduction. *Science*, *268*(5208), 247-251.
- Morse-Gaudio, M., Connolly, J. M., & Rose, D. P. (1998). Protein kinase C and its isoforms in human breast cancer cells: relationship to the invasive phenotype. *International journal of oncology*, *12*(6), 1349-1403.
- Mosior, M., & McLaughlin, S. (1991). Peptides that mimic the pseudosubstrate region of protein kinase C bind to acidic lipids in membranes. *Biophysical journal*, *60*(1), 149.
- Murray, N. R., Baumgardner, G. P., Burns, D. J., & Fields, A. P. (1993). Protein kinase C isotypes in human erythroleukemia (K562) cell proliferation and differentiation. Evidence that beta II protein kinase C is required for proliferation. *Journal of Biological Chemistry*, *268*(21), 15847-15853.
- Nahon, P., & Zucman-Rossi, J. (2012). Single nucleotide polymorphisms and risk of hepatocellular carcinoma in cirrhosis. *Journal of hepatology*, *57*(3), 663-674.
- Newton, A. C. (2018). *Protein kinase C as a tumor suppressor*. Paper presented at the Seminars in cancer biology.
- Newton, A. C. J. C. r. (2001). Protein kinase C: structural and spatial regulation by phosphorylation, cofactors, and macromolecular interactions. *101*(8), 2353-2364.
- Nguyen, T. A., Boyle, D. L., Wagner, L. M., Shinohara, T., & Takemoto, D. J. (2003). LEDGF activation of PKC γ and gap junction disassembly in lens epithelial cells. *Exp Eye Res*, *76*(5), 565-572. doi:10.1016/s0014-4835(03)00049-6
- Nishizuka, Y. (1992). Intracellular signaling by hydrolysis of phospholipids and activation of protein kinase C. *Science*, *258*(5082), 607-614.
- Oller, A. R., Rastogi, P., Morgenthaler, S., & Thilly, W. G. (1989). A statistical model to estimate variance in long term-low dose mutation assays: testing of the model in a

- human lymphoblastoid mutation assay. *Mutat Res*, 216(3), 149-161.
doi:10.1016/0165-1161(89)90001-0
- Parker, P. J., & Parkinson, S. J. (2001). AGC protein kinase phosphorylation and protein kinase C. *Biochem Soc Trans*, 29(Pt 6), 860-863. doi:10.1042/0300-5127:0290860
- Parsons, M., & Adams, J. C. (2008). Rac regulates the interaction of fascin with protein kinase C in cell migration. *Journal of cell science*, 121(17), 2805-2813.
- Pejaver, V., Urresti, J., Lugo-Martinez, J., Pagel, K. A., Lin, G. N., Nam, H.-J., . . . Iakoucheva, L. M. J. B. (2017). MutPred2: inferring the molecular and phenotypic impact of amino acid variants. 134981.
- Peters, K. G., Marie, J., Wilson, E., Ives, H. E., Escobedo, J., Del Rosario, M., . . . Williams, L. T. (1992). Point mutation of an FGF receptor abolishes phosphatidylinositol turnover and Ca²⁺ flux but not mitogenesis. *Nature*, 358(6388), 678-681.
- Petukh, M., Kucukkal, T. G., & Alexov, E. (2015). On human disease-causing amino acid variants: Statistical study of sequence and structural patterns. *Human mutation*, 36(5), 524-534.
- Podar, K., Raab, M. S., Zhang, J., McMillin, D., Breitzkreutz, I., Tai, Y.-T., . . . Chauhan, D. (2007). Targeting PKC in multiple myeloma: in vitro and in vivo effects of the novel, orally available small-molecule inhibitor enzastaurin (LY317615. HCl). *Blood*, 109(4), 1669-1677.
- Quang, D., Chen, Y., & Xie, X. J. B. (2015). DANN: a deep learning approach for annotating the pathogenicity of genetic variants. 31(5), 761-763.
- Rentzsch, P., Witten, D., Cooper, G. M., Shendure, J., & Kircher, M. J. N. a. r. (2019). CADD: predicting the deleteriousness of variants throughout the human genome. 47(D1), D886-D894.
- Ritchie, G. R., Dunham, I., Zeggini, E., & Flicek, P. J. N. m. (2014). Functional annotation of noncoding sequence variants. 11(3), 294-296.
- Rosenberg, M., & Ravid, S. (2006). Protein kinase C γ regulates myosin IIB phosphorylation, cellular localization, and filament assembly. *Molecular biology of the cell*, 17(3), 1364-1374.
- Roy, A., Kucukural, A., & Zhang, Y. (2010). I-TASSER: a unified platform for automated protein structure and function prediction. *Nature protocols*, 5(4), 725-738.
- S Darvesh, A., B Aggarwal, B., & Bishayee, A. (2012). Curcumin and liver cancer: a review. *Current pharmaceutical biotechnology*, 13(1), 218-228.
- Sabater, L., Bataller, L., Carpentier, A. F., Aguirre-Cruz, M., Saiz, A., Benyahia, B., . . . Graus, F. (2006). Protein kinase C γ autoimmunity in paraneoplastic cerebellar degeneration and non-small-cell lung cancer. *Journal of Neurology, Neurosurgery & Psychiatry*, 77(12), 1359-1362.
- Saito, N., & Shirai, Y. (2002). Protein kinase C γ (PKC γ): function of neuron specific isotype. *The Journal of Biochemistry*, 132(5), 683-687.
- Shackelford, D. B., & Shaw, R. J. (2009). The LKB1-AMPK pathway: metabolism and growth control in tumour suppression. *Nature Reviews Cancer*, 9(8), 563-575.
- Shihab, H. A., Gough, J., Mort, M., Cooper, D. N., Day, I. N., & Gaunt, T. R. J. H. g. (2014). Ranking non-synonymous single nucleotide polymorphisms based on disease concepts. 8(1), 1-6.
- Shin, H. R., Oh, J. K., Masuyer, E., Curado, M. P., Bouvard, V., Fang, Y., . . . Hong, S. T. (2010). Comparison of incidence of intrahepatic and extrahepatic cholangiocarcinoma--focus on East and South-Eastern Asia. *Asian Pac J Cancer Prev*, 11(5), 1159-1166.

- Smith, A. M., Bowers, B. J., Radcliffe, R. A., & Wehner, J. M. (2006). Microarray analysis of the effects of a γ -protein kinase C null mutation on gene expression in striatum: a role for transthyretin in mutant phenotypes. *Behavior genetics*, *36*(6), 869-881.
- Smith, M. R., DeGudicibus, S. J., & Stacey, D. W. (1986). Requirement for c-ras proteins during viral oncogene transformation. *Nature*, *320*(6062), 540-543.
- Takahashi, T., Ueno, H., & Shibuya, M. (1999). VEGF activates protein kinase C-dependent, but Ras-independent Raf-MEK-MAP kinase pathway for DNA synthesis in primary endothelial cells. *Oncogene*, *18*(13), 2221-2230.
- Takai, Y., Kishimoto, A., Inoue, M., & Nishizuka, Y. (1977). Studies on a cyclic nucleotide-independent protein kinase and its proenzyme in mammalian tissues. I. Purification and characterization of an active enzyme from bovine cerebellum. *Journal of Biological Chemistry*, *252*(21), 7603-7609.
- Takai, Y., Kishimoto, A., Iwasa, Y., Kawahara, Y., Mori, T., & Nishizuka, Y. (1979). Calcium-dependent activation of a multifunctional protein kinase by membrane phospholipids. *J Biol Chem*, *254*(10), 3692-3695.
- Takai, Y., Kishimoto, A., Kikkawa, U., Mori, T., & Nishizuka, Y. (1979). Unsaturated diacylglycerol as a possible messenger for the activation of calcium-activated, phospholipid-dependent protein kinase system. *Biochemical and biophysical research communications*, *91*(4), 1218-1224.
- Tarao, K., Rino, Y., Ohkawa, S., Shimizu, A., Tamai, S., Miyakawa, K., . . . Okamoto, N. J. C. (1999). Association between high serum alanine aminotransferase levels and more rapid development and higher rate of incidence of hepatocellular carcinoma in patients with hepatitis C virus-associated cirrhosis. *86*(4), 589-595.
- Thomas, R., McConnell, R., Whittacker, J., Kirkpatrick, P., Bradley, J., & Sandford, R. (1999). Identification of mutations in the repeated part of the autosomal dominant polycystic kidney disease type 1 gene, PKD1, by long-range PCR. *The American Journal of Human Genetics*, *65*(1), 39-49.
- Tyson, G. L., & El-Serag, H. B. (2011). Risk factors for cholangiocarcinoma. *Hepatology*, *54*(1), 173-184. doi:10.1002/hep.24351
- Venselaar, H., Te Beek, T. A., Kuipers, R. K., Hekkelman, M. L., & Vriend, G. J. B. b. (2010). Protein structure analysis of mutations causing inheritable diseases. An e-Science approach with life scientist friendly interfaces. *11*(1), 1-10.
- Vivanco, I., & Sawyers, C. L. (2002). The phosphatidylinositol 3-kinase–AKT pathway in human cancer. *Nature Reviews Cancer*, *2*(7), 489-501.
- Wallace, A. C., Laskowski, R. A., Thornton, J. M. J. P. e., design, & selection. (1995). LIGPLOT: a program to generate schematic diagrams of protein-ligand interactions. *8*(2), 127-134.
- Wang, X., Lu, X. A., Song, X., Zhuo, W., Jia, L., Jiang, Y., & Luo, Y. (2012). Thr90 phosphorylation of Hsp90 α by protein kinase A regulates its chaperone machinery. *Biochem J*, *441*(1), 387-397. doi:10.1042/bj20110855
- Webb, B. L., Hirst, S. J., & Giembycz, M. A. (2000). Protein kinase C isoenzymes: a review of their structure, regulation and role in regulating airways smooth muscle tone and mitogenesis. *British journal of pharmacology*, *130*(7), 1433.
- Wilkinson, S. E., Parker, P., & Nixon, J. (1993). Isoenzyme specificity of bisindolylmaleimides, selective inhibitors of protein kinase C. *Biochemical Journal*, *294*(2), 335-337.
- Wright, A. F. J. e. L. (2001). Genetic variation: polymorphisms and mutations.
- Yamaguchi, Y., Shirai, Y., Matsubara, T., Sanse, K., Kuriyama, M., Oshiro, N., . . . Saito, N. (2006). Phosphorylation and up-regulation of diacylglycerol kinase gamma via its

- interaction with protein kinase C gamma. *J Biol Chem*, 281(42), 31627-31637. doi:10.1074/jbc.M606992200
- Yang, J., Song, X., Chen, Y., Lu, X. a., Fu, Y., & Luo, Y. (2014). PLC γ 1–PKC γ Signaling-Mediated Hsp90 α Plasma Membrane Translocation Facilitates Tumor Metastasis. *Traffic*, 15(8), 861-878.
- Yoon, Y. J., Chang, H. Y., Ahn, S. H., Kim, J. K., Park, Y. K., Kang, D. R., . . . Chon, C. Y. (2008). MDM2 and p53 polymorphisms are associated with the development of hepatocellular carcinoma in patients with chronic hepatitis B virus infection. *Carcinogenesis*, 29(6), 1192-1196.
- Young, L. H., Balin, B. J., & Weis, M. T. (2005). Gö 6983: a fast acting protein kinase C inhibitor that attenuates myocardial ischemia/reperfusion injury. *Cardiovasc Drug Rev*, 23(3), 255-272. doi:10.1111/j.1527-3466.2005.tb00170.x
- Zeidman, R., Pettersson, L., Sailaja, P. R., Truedsson, E., Fagerström, S., Pålman, S., & Larsson, C. (1999). Novel and classical protein kinase C isoforms have different functions in proliferation, survival and differentiation of neuroblastoma cells. *International journal of cancer*, 81(3), 494-501.
- Zhang, L., Huang, J., Yang, N., Liang, S., Barchetti, A., Giannakakis, A., . . . Roby, K. F. (2006). Integrative genomic analysis of protein kinase C (PKC) family identifies PKC ϵ as a biomarker and potential oncogene in ovarian carcinoma. *Cancer research*, 66(9), 4627-4635.
- Zhang, Y., Hu, X., Wang, H.-K., Shen, W.-W., Liao, T.-Q., Chen, P., & Chu, T.-W. (2014). Single-nucleotide polymorphisms of the PRKCG gene and osteosarcoma susceptibility. *Tumor Biology*, 35(12), 12671-12677.
- Zhong, X., Zhang, H., Zhu, Y., Liang, Y., Yuan, Z., Li, J., . . . He, T. J. M. c. (2020). Circulating tumor cells in cancer patients: Developments and clinical applications for immunotherapy. *19(1)*, 1-12.
- Zhou, T., Song, L., Yang, P., Wang, Z., Lui, D., & Jope, R. S. (1999). Bisindolylmaleimide VIII facilitates Fas-mediated apoptosis and inhibits T cell-mediated autoimmune diseases. *Nat Med*, 5(1), 42-48. doi:10.1038/4723
- Zidovetzki, R., & Lester, D. S. (1992). The mechanism of activation of protein kinase C: a biophysical perspective. *Biochimica et Biophysica Acta (BBA)-Molecular Cell Research*, 1134(3), 261-272.